ELSEVIER

Journal of Structural Geology 27 (2005) 1577–1598

JOURNAL OF STRUCTURAL GEOLOGY

www.elsevier.com/locate/jsg

Influence of *P/T* conditions on the style of normal fault initiation and growth in limestones from the SE-Basin, France

L. Micarelli[a,*], A. Benedicto[a], C. Invernizzi[b], B. Saint-Bezar[a], J.L. Michelot[a], P. Vergely[a]

[a]*Department Science de la Terre, Groupe Dyn. Syst. Faillés, UMR 7072, Université Paris Sud XI, 91405 Orsay, France*
[b]*Department of Earth Science, University of Camerino, Via Gentile III da Varano, 62032 Camerino, Italy*

Received 7 December 2004
Available online 20 July 2005

Abstract

A conventional and cathodoluminescence microscopy, stable isotope, and fluid inclusion study was undertaken on normal fault zones exposed on vertical cliffs in Tithonian limestones of the French SE-Basin. The aim was to determine the chronology of deformation, and factors controlling normal fault nucleation and evolution in carbonate rocks. Two models are proposed for fault zone development depending on the depths at which deformation takes place. At depths of 3–3.5 km, incipient shear zones consist of en-échelon veins, filled by fibrous calcite and confined to limestone layers bounded by thin clayey interlayers. As deformation increases and the layers rotate, slip occurs along the clay-rich interlayers. A system of pull-aparts forms allowing displacement to increase. Pull-aparts are commonly filled by fibrous calcite crystals. At depths of 1.5–2 km, faults initiate as small slip surfaces, early nucleating in some limestone layers. Their propagation is impeded by thin clayey interlayers, which enhances fracturing and bending of the limestone layers. As slip surfaces propagate, they overlap and can connect with one another by means of dilational jogs that are filled by large euhedral calcite crystals. In the first case, pull-aparts are coupled with the solution seams that reuse preexisting, rotated clay-rich interlayers. As they formed, they progressively filled and the fluid circulation remained local. In the second case, longer slip planes connect by dilation jogs, that are not immediately filled, which enhance the circulation of fluids, which show chemical variations. It appears that *P/T* conditions strongly control the relative role of brittle processes and solution/crystallization mechanisms, and the style of the early stages of normal faulting in the same limestone rocks.

Keywords: Normal fault; Fault initiation; Pull-apart; Dilational jog; Pressure solution; Limestone

1. Introduction

In recent years, the style and the processes of fault nucleation have been investigated in both natural fault zones and experimental models of the mechanics of shear failure (e.g. Franssen et al., 1994; Maltman, 1994; Moore and Lockner, 1995; Menendez et al., 1996). Despite several works describing the style of fault initiation, few field studies have been undertaken to describe incipient normal faults in limestone rocks and to determine how such faults nucleate and grow (e.g. Peacock and Sanderson, 1991; Peacock and Zhang, 1994). Relevant studies on strike-slip fault nucleation are those of Peacock and Sanderson (1995), Willemse et al. (1997) and Kelly et al. (1998). Crider and Peacock (2004) give a review of field observation on initiation of faults and the relationships between normal en-échelon vein arrays and shear displacement have been investigated by Mazzoli and Di Bucci (2003) and Mazzoli et al. (2004). Nevertheless, little attention has been paid to the microstructural characteristics of normal fault-related structures and to the influence of depth on the style of deformation. Depth, and thus the *P/T* conditions, controls the relative role of brittle and physicochemical processes, and thus the fault-rock properties (Knipe, 1997; Hesthammer and Fossen, 2000).

The purpose of this paper is to describe the nucleation and the early stages of growth of normal fault zones in Tithonian limestone rocks, in the SE-Basin of the French Alps. Most of the studied faults occur in two main survey sites, and are exposed on natural vertical cliff faces that allow the study of vertical segmentation and evolution of normal faults. Microstructural analyses were undertaken to

* Corresponding author. Tel.: +33 169154901.
E-mail address: luca.micarelli@geol.u-psud.fr (L. Micarelli).

0191-8141/$ - see front matter © 2005 Elsevier Ltd. All rights reserved.
doi:10.1016/j.jsg.2005.05.004

define the relative chronology of the different structures and to establish the deformation mechanisms responsible for their development. Stable isotope analysis was carried out to characterize the fluids circulating through the fault zones. The *P*/*T* conditions during the deformation were investigated by means of fluid inclusions analysis. Based on the integration of structural and geochemical analysis of deformation features and cements, on the fault-zone geometry and its hierarchical evolution, we propose a model for the development of normal fault zones in the studied limestones and discuss the role of depth and the related *P*/*T* conditions on the style of deformation.

2. Geological setting

The SE-Basin in France (Fig. 1a) was one of the most subsident areas of the Mesozoic Tethyan passive margin (Dercourt et al., 1993; De Graciansky et al., 1993). The Upper Jurassic deposits form a thick marl–limestone succession, prograding from the inner shelf-barrier domain to the outer mud-dominated shelf, during the Kimmeridgian and Tithonian times. In the centre of the basin, the uppermost part of the succession forms a 20–200-m-thick cliff, informally called the 'Barre Tithonique' (Gignoux and Moret, 1938), which is composed of coarse carbonate breccia bodies, interbedded with calcarenites and marl–lime mudstones. Some calcarenites were interpreted by Séguret et al. (2001) as tempestites, resulting from transport and deposition of carbonate sands under wave-induced combined flow. The coarse breccias are the result of the in-situ brecciation of cohesive lime mud by heterogeneous liquefaction during the worst weather periods (Bouchette et al., 2001). The base of the 'Barre Tithonique' is either Late Kimmeridgian or Tithonian in age, with the uppermost part of this unit being Late Tithonian to Early Berriasian (Bouchette et al., 2001).

The 'Barre Tithonique' is affected by a system of normal faults with throws of up to a few metres. This system is related to a weak extensional phase with a general WNW–ENE direction of extension, as shown by the palaeostress analysis (Fig. 1b). The fault dip angles are coherent with one extensional phase affecting the limestone series before the Alpine contraction (i.e. ante-Miocene) and the related thrusting and bending. The age of this fault system is not well-constrained but stratigraphic data suggest it is Upper Cretaceous. Although some of the faults have been reactivated during the Alpine compression, mainly in strike-slip motion, the faults studied in this work do not show any evidence of reactivation.

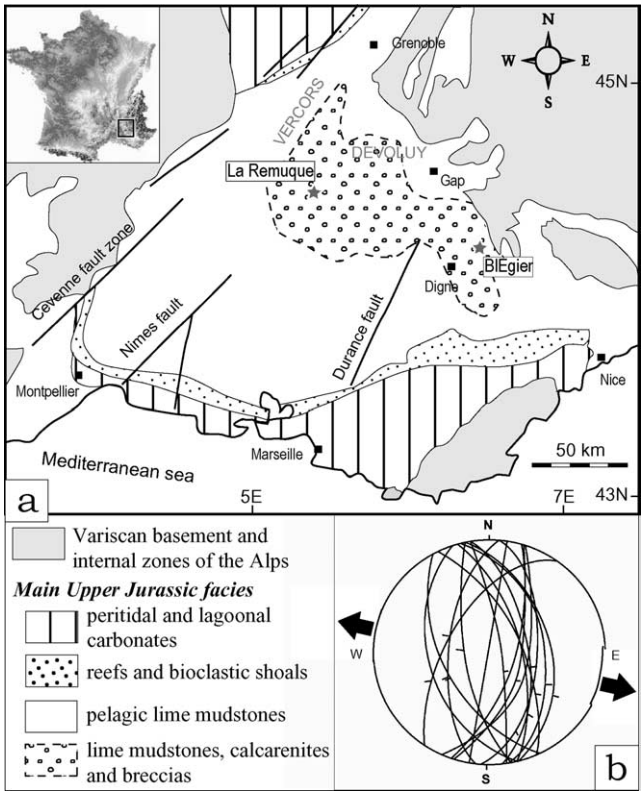

Fig. 1. (a) Simplified geological map of the South East Basin in France (from Séguret et al., 2001) showing the overall distribution of the main carbonate Upper Jurassic facies. The two studied sites are shown. (b) Orientation diagram (Schmidt projection, lower hemisphere) of the normal faults affecting the 'Barre Titonique' and palaeostress orientation analysis.

We focused our study on several fault zones cropping out in two sites: Blégier and La Remuque (location in Fig. 1a). In both sites, the studied faults affect the 'Barre Tithonique' at the same stratigraphic level, showing very similar lithology features and consisting of mainly mudstones alternated with fine calcarenites. Clayey interlayers, a few millimetres thick, are present. Currently, the complete Cretaceous series overlaying the 'Barre Tithonique' and cropping out in the two studied sites have a difference of at least 700 m in thickness (Ballesio et al., 1975; Debrand-Passard and Courbouleix, 1984; Haccard et al., 1989). The upper part of the Cretaceous series in the Blégier site is more reduced by erosion (Haccard et al., 1989). The burial history, reconstructed by K/Ar dating (Cros et al., 1993) and basin modelling (Roure et al., 1994), indicates maximum burial of the SE-Basin series at about 120 Ma. At that time, Triassic evaporates (laying 4–5 km under the Tithonian limestone) were buried to a depth of 3.7 km in the west of the SE-Basin (about 60 km west to the La Remuque site),

Fig. 2. Polished surfaces of some vertical outcrops studied in this work. (a) Blégier: fault zones are characterized by arrays of short slip surfaces and mostly calcite-filled pull-aparts. The fault in the picture has a displacement of 25 cm. (b) Another studied fault showing a bigger displacement (≈80 cm). (c) La Remuque: fault zones show relatively long slip surfaces connected by calcite-filled dilational jogs. The locations of the oriented sample cores collected for microstructural analyses are shown.

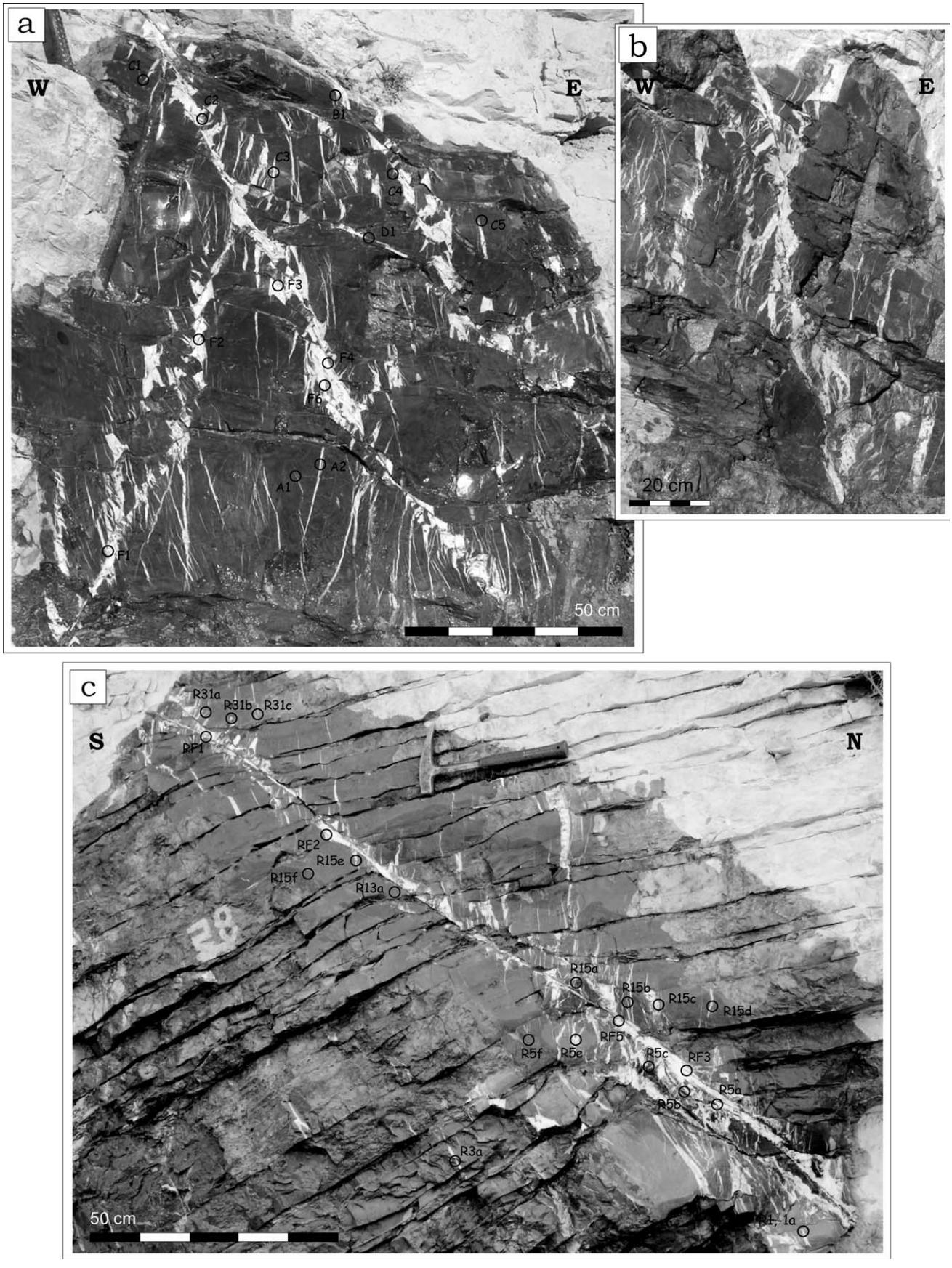
a
W
E
C1
C2
B1
C3
C4
C5
D1
F3
F2
F4
F5
A2
A1
F1
50 cm
b
W
E
20 cm
c
S
N
R31a
R31b
R31c
RF1
RE2
R15e
R15f
R13a
R15a
R15b
R15c
R15d
RF5
R5f
R5e
R5c
RF3
R5a
R5b
R3a
R1,-1a
50 cm

whereas, according to geodynamic reconstructions, the same horizons were buried at more than 8 km in the east (Guilhaumou et al., 1996), towards the Blégier site. During the Late Cretaceous to Tertiary episodes of compression, a regional uplift occurred, inducing 1.5–2 km of erosion in the Cretaceous sequences in the SE-Basin (Guilhaumou et al., 1996, and references therein).

In the Blégier site, the 'Barre Tithonique' dips 20–30° to the E. In this paper a fault oriented N020/75°/E is taken as a selected example (Fig. 2a). The displacement is approximately 25 cm. The slip vector, based on the striae on the fault plane, has a pitch of 75° SE. In the same site, we also studied faults with up to 100 cm displacement for comparing microstructural data (e.g. the fault shown in Fig. 2b). In the La Remuque site, the 'Barre Tithonique' dips approximately 10–20° to the SE. The studied faults show a general strike direction of N050–N080°. A fault oriented N055/30°/NW is used as a selected example, with a displacement of 80 cm (Fig. 2c). The striae on the fault plane show pure dip-slip.

3. Methods

Large portions (areas comprised of between 2 and 3 m^2) of some studied fault zones were mechanically polished by means of a portable electric sander, in order to improve the quality of the exposure and outline microstructures (Fig. 2). Particular attention was paid to the cross-cutting relationships between the calcite-filled fractures, the solution seams and the slip planes. Forty-three oriented sample cores were collected with a portable rock drill and 70 thin sections of the various fracture systems and host-rock were produced, including sections cut perpendicularly to the fault plane and parallel to the slip direction, and/or to the examined microstructure.

Petrographic examination of thin sections using transmitted light microscopy was used to determine the mineralogy, texture, and paragenesis of the microstructures, and the time relationships not recognizable at the macroscale analysis. Cathodoluminescence (CL) microscopy was used to identify compositional zoning (Marshall, 1988; Pagel et al., 2000) and cross-cutting relations between vein minerals not apparent in transmitted light. CL microscopy was carried out with a Cold Cathodoluminescence Model (Technosyn 8200 M411) at 12–16 kV and 450–550 μA gun current.

Samples of the veins and host-rock were drilled from the polished surfaces of samples to determine their carbon and oxygen isotopic composition on a VG Sira mass spectrometer. The powdered carbonate samples were reacted with orthophosphoric acid under vacuum at 25 °C (Craig, 1957). Isotope data are expressed as per mil (‰) deviation, δ, from the Vienna Pee Dee Belemnite (VPDB) standard. Reproducibility is better than 0.1‰ for both $\delta^{13}C$ and $\delta^{18}O$.

Fluid inclusion studies were performed on doubly polished wafers 150 μm thick. Petrographic analysis for identification of fluid inclusion origin and distribution, and ratio of vapour to liquid, was conducted with a Leitz Ortolux Optical microscope with long-way objectives. Fluid inclusion microthermometry was performed on a USGS heating-freezing stage. The homogenization temperature (T_h) was reproducible between 0 and 650 °C with a confidence of ± 1 °C. Confidence for the final melting temperature of ice (T_m ice) is 0.1 °C. Instrument calibration with standards by Fluid Inc. (Denver, Colorado) was performed using three known points (H_2O melting and triple points and CO_2 melting point). Observations were made on fluid inclusions interpreted as being primary in origin (Goldstein and Reynolds, 1994). Re-equilibration of fluid inclusions to lower densities, inducing higher T_h, may occur during intracrystalline deformation of crystals, but petrographic analysis was performed to avoid this problem. Thermometric measurements were made in the vicinity of the less strained zones of the crystals. Strongly deformed zones (e.g. intensely twinned zones in calcite) were avoided to minimize the analysis of stretched or leaked fluid inclusions.

4. Deformation features and fracture petrology in the Blégier and La Remuque sites

Macro- and micro-structural analyses allow various types of fractures, their petrology and their cross-cutting relationships to be distinguished. Each type of fracture can be associated with a deformation episode in the development of the fault zone. At both studied sites, the Tithonian limestones are uniformly affected by randomly-oriented calcite veins, a few tens of micrometres thick, perpendicular to the bedding, and by stylolite surfaces mostly sub-parallel to the stratification boundaries. These structures are cut by all other observed (tectonic) fractures and do not show any spatial relationships with the studied faults, which suggests an early (diagenetic) origin, probably related to the compaction of the sedimentary series. Note that in the

Fig. 3. Detailed images from the Blégier site. (a) Adjacent pull-aparts connected by interlayer-derived slip surfaces (black arrows). The irregular shapes of slip surfaces suggest combined shear and pressure solution. Pull-aparts allow displacement to increase along the fault zone. Note the 'tails' (white arrows) at opposite corners sheared off by pull-apart opening (polished surface picture). (b) Slip surface between two pull-aparts. Pull-aparts are filled by mostly fibrous calcite crystals displaying a typical grey colour. (c) Slip surface detail: alternation of fibrous calcite crystals and fine clay beds. (d) Slip surfaces (white arrows) display irregular shapes with (e) stylolitic peaks (black arrows) and abundant clayey material (white arrow). (b), (d) and (e): crossed polarized photomicrographs; (c): plain light photomicrograph.

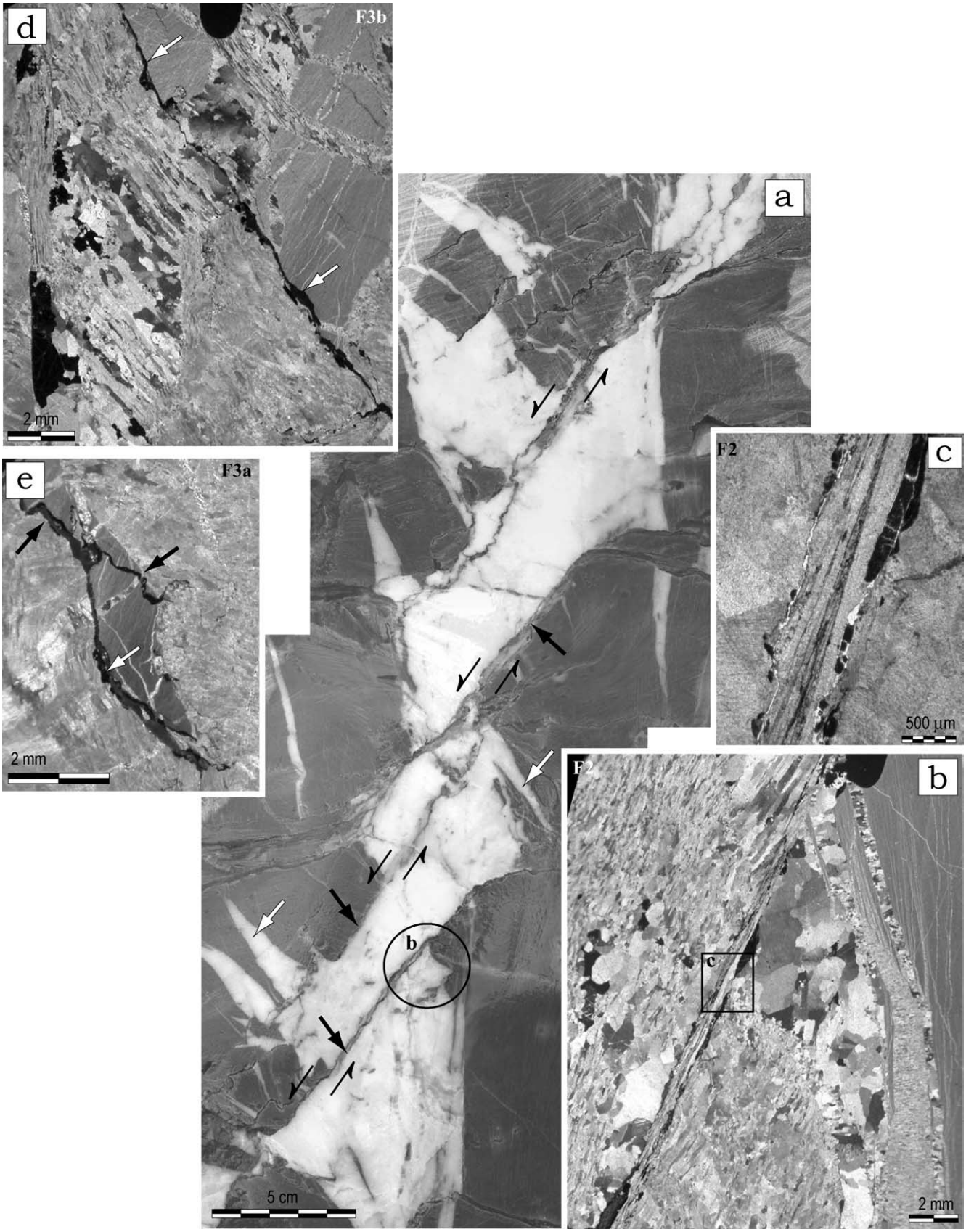
d
F3b
2 mm
a
e
F3a
2 mm
F2
c
500 μm
b
5 cm
F2
b
c
2 mm

following paragraphs the terms 'Type 1' and 'Type 2' fractures are simply descriptive.

4.1. The Blégier faults

4.1.1. Slip surfaces

In the Blégier site, fault zones are characterized by short slip surfaces (a few centimetres in length) overlapping and following one another in a dense array (Figs. 2a and 3a). Bedding is deflected and thinned in the fault zone, and the deflected clay-rich interlayers appear to localize slip. Slip surfaces rarely cross through the limestone layers, but connect and bound adjacent pull-apart structures (e.g. Peacock and Zhang, 1994; Willemse et al., 1997; Section 4.1.2), which let some dragged and disconnected layers seem to keep their continuity across the fault zone.

Slip surfaces display evidence for combined shear and pressure solution (Fig. 3a, d and e). The two processes, pressure solution and slip, may coexist on the same surface linking pull-aparts (Peacock and Sanderson, 1995). Shear is testified in places by the presence of fibrous calcite crystals parallel to the slip vector, commonly associated with fine clay beds to form alternations a few millimetres thick (Fig. 3b and c). The calcite fibres constitute the striae on slip surfaces. Thin section analysis outlines a strong concentration of clayey material in all the interlayer-derived slip surfaces that display irregular shapes with stylolitic peaks testifying that the pressure solution processes played a major role in their development (Fig. 3d and e). Pressure solution processes appear to be earlier than slip, with fibrous calcite on slip surfaces being more abundant as fault zone displacement increases. Under CL microscopy, fibrous calcite on slip surfaces displays the same red luminescence as the host-limestone (see later Fig. 6a).

4.1.2. Pull-aparts

Extensional fractures between overlapping slip surfaces or stepped fault segments have been described by several authors (e.g. Sibson, 1989; Willemse et al., 1997, and references therein). These fractures show significant differences between the two studied sites. According to their different geometries, genesis and role played during deformation (see later Section 7.2.3), in this paper we will call 'pull-aparts' (following Willemse et al., 1997) the structures characterizing faults at the Blégier site and 'dilational jogs' (following Sibson, 1989) those characterizing faults at the La Remuque site (Section 4.2.2).

Linked pull-aparts are the most important features in developing the Blégier fault segmentation (Figs. 2a and 3a). They connect the layers' ends, dragged and disconnected by the deformation. They appear therefore to be restricted within each limestone layer and are limited, at the top and the bottom, by the clayey interlayers. The interlayers appear to have been rotated and are affected by pressure solution and shear phenomena. The interlayer-derived fractures, connecting two adjacent pull-aparts, are the slip surfaces described in the Section 4.1.1. Slip, coupled with solution processes, on these fractures allow displacement to increase along the fault zone. In places, well-developed pull-aparts show 'tail' structures at opposite corners (Fig. 3a), sheared off by the associated pull-apart (Willemse et al., 1997). The Blégier pull-aparts show geometries similar to those described by McCoss (1986) and Peacock and Sanderson (1995) for simple shear fault zones, considering the angles between the pull-apart longitudinal axes, the infinitesimal displacement and the fault zone boundary.

Pull-aparts are filled mostly by elongated, commonly fibrous calcite crystals, displaying curved and serrated boundaries and a typical dark-grey colour in plain-light microscopy (Fig. 3b and d). They testify several steps of 'crack-seal' filling. The presence of syntectonic fibrous crystals suggests a low ratio of crystal growth velocity versus opening velocity (Hilgers and Urai, 2002). Some large (up to 1 mm in width), subhedral crystals are present, showing intense development of thin twin planes and, in places, thick (Type II of Burkhard, 1993), rarely curved twin lamellae indicating significant deformation. Undulatory extinction is present in places. Both fibrous and large calcite crystals filling the pull-aparts show the same uniform red CL-luminescence as the host-limestone (see later Fig. 6b).

4.1.3. Type 1 fractures

Type 1 fractures are 1–10 mm in width, are perpendicular to the layer boundaries and rarely cut them (Fig. 4a). They show strike-directions parallel to the fault strikes and affect the whole limestone rock. They appear to be passively rotated within the dragged layers into the fault zone. They are planar, have straight boundaries and show a central portion that tapers off into narrow tails (Fig. 4a).

Type 1 fractures comprise large euhedral–subhedral crystals (1–5 mm wide) with straight grain boundaries. All the crystals display thin twinning and twin lamellae are straight. Veins show antitaxial growth and open perpendicularly to their walls, as testified by displaced early stylolite surfaces (Fig. 4b). They commonly display a medial line consisting of aligned limestone fragments and small calcite crystals. The calcite filling in Type 1 fractures displays very

Fig. 4. Blégier site. (a) Type 1 fractures (black arrows) are cut by Type 2 fractures (white arrows) and (b) display large euhedral–subhedral twinned crystals. Cut old stylolite surfaces (black arrows) show that fractures opened perpendicularly to their walls. (c) Type 2 fractures (black arrows) are commonly organized en-échelon defining shear zones. (d) They are filled mainly by fibrous calcite crystals growing at low angles to the fractures walls (white arrows). (e) A Type 2 fracture is cut and dissolved by a stylolite reactivating a clay-rich interlayer. In places, recrystallization phenomena lead to the nucleation of preferentially oriented grains (white arrow). (a) and (c): polished outcrop pictures; (b), (d) and (e): crossed polarized photomicrographs.


a
2 cm

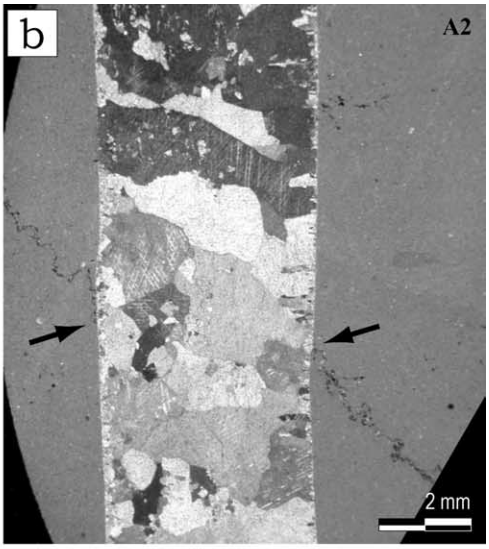
b
A2
2 mm

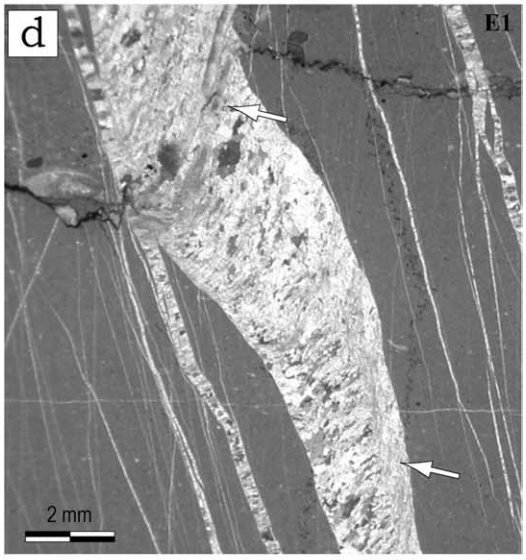
d
E1
2 mm


c
0
5 cm

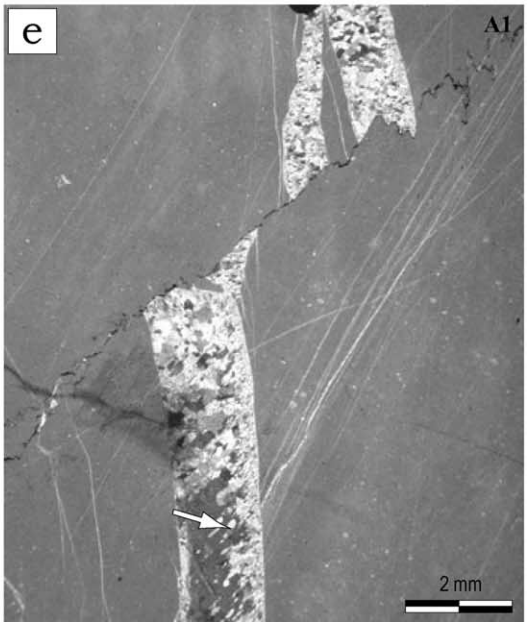
e
A1
2 mm

uniform dull-orange or red luminescence on CL microscopy, just a little weaker (darker) than the host-limestones (see later Fig. 6c).

4.1.4. Type 2 fractures

Type 2 fractures are sub-vertical, but show different dip angles with respect to the Type 1 fractures and cut them (Fig. 4a). They do not cross through the layer boundaries. They are commonly en-échelon, defining shear zones sub-parallel, synthetic or antithetic, to the faults (Fig. 4c). In a few cases they show a sigmoidal shape, probably caused by rotation of their central part as a result of shearing (Ramsay and Graham, 1970). The shear zones affect the whole limestone rock and only in places are associated with the development of a fault zone.

In Type 2 fractures, elongated, commonly fibrous crystals are the most common features, showing slightly curved and serrated fibre grain boundaries. Calcite fibres grew at low angles to the fracture walls (Fig. 4d). Large, twinned, euhedral crystals (as in Type 1 fractures) are rarely present, but they are commonly affected by the nucleation of new small, preferentially oriented grains (Fig. 4e). These are probably related to localized recrystallization phenomena that could have affected the large crystals of the older Type 1 fractures. Calcite filling Type 2 fractures displays the same uniform, red CL-luminescence as the host-limestone (see Fig. 6d).

4.1.5. Stylolitic surfaces

Most pressure solution phenomena are concentrated on slip surfaces (Sections 4.1.1 and 4.1.2) bounding the pull-aparts and appear to be strictly coupled with their development. Other late solution seams exist, but they usually reactivated early, compaction-related stylolites and the clay-rich interlayers (Fig. 4d and e). In this case, stylolites that are cut and displaced by a calcite-filled fracture appear to dissolve the fracture (e.g. Fig. 4d). These features indicate that early stylolites, maintaining a suitable orientation relative to vertical loading, were also reactivated during extensional deformation (see also Mazzoli and Di Bucci, 2003). However, the strong concentration of the solution seams near to the slip surfaces, where the limestone layers appear dragged and strongly thinned, suggests that pressure solution processes are likely to be related to the local increase and layering-controlled reorientation of the maximum principal compressive stress direction rather than to the far-field extension-related stress.

4.1.6. Fractures with baroque dolomite

Baroque dolomite (e.g. Alsharhan and Williams, 1987) is present in many samples from the survey site. It displays large (some millimetres wide) fan-shape crystals, curved crystal faces and undulatory extinction (Fig. 5a). Crystals show fine cleavage and are affected by a system of microfractures along the planes of cleavage. The fractures containing baroque dolomite systematically appear red to yellow in colour in outcrop and under optical microscopy. Under CL microscopy, the baroque dolomite is dark-brown to non-luminescent (Fig. 6e).

The baroque dolomite partially replaces mostly the large euhedral calcite crystals in Type 1 fractures and is rarely present in Type 2 fractures. In places, dolomite is located where the calcite fractures cross the stylolitic surfaces (Fig. 5b), and fills reopened stylolite segments (Fig. 6e). Moreover, large baroque dolomite areas are present in the largest pull-aparts. In all cases, calcite and dolomite crystals coexist and are mixed within the same part of the fractures. This suggests that the baroque dolomite is related to recrystallization processes. Note that baroque dolomite constitutes an indicator of crystallization at temperatures

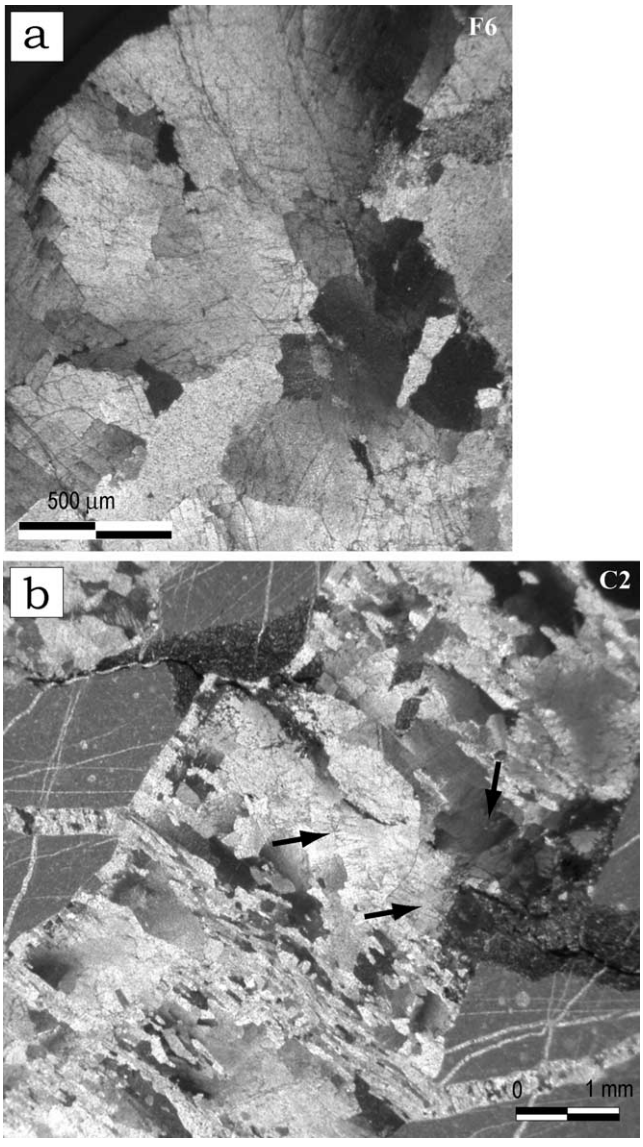

Fig. 5. Blégier site. (a) Large baroque dolomite crystals display a typical fan-shape, curved faces and undulatory extinction. (b) Recrystallization-related baroque dolomite crystals (black arrows) located where the calcite fracture cross stylolitic surfaces. Crossed polarized photomicrographs.

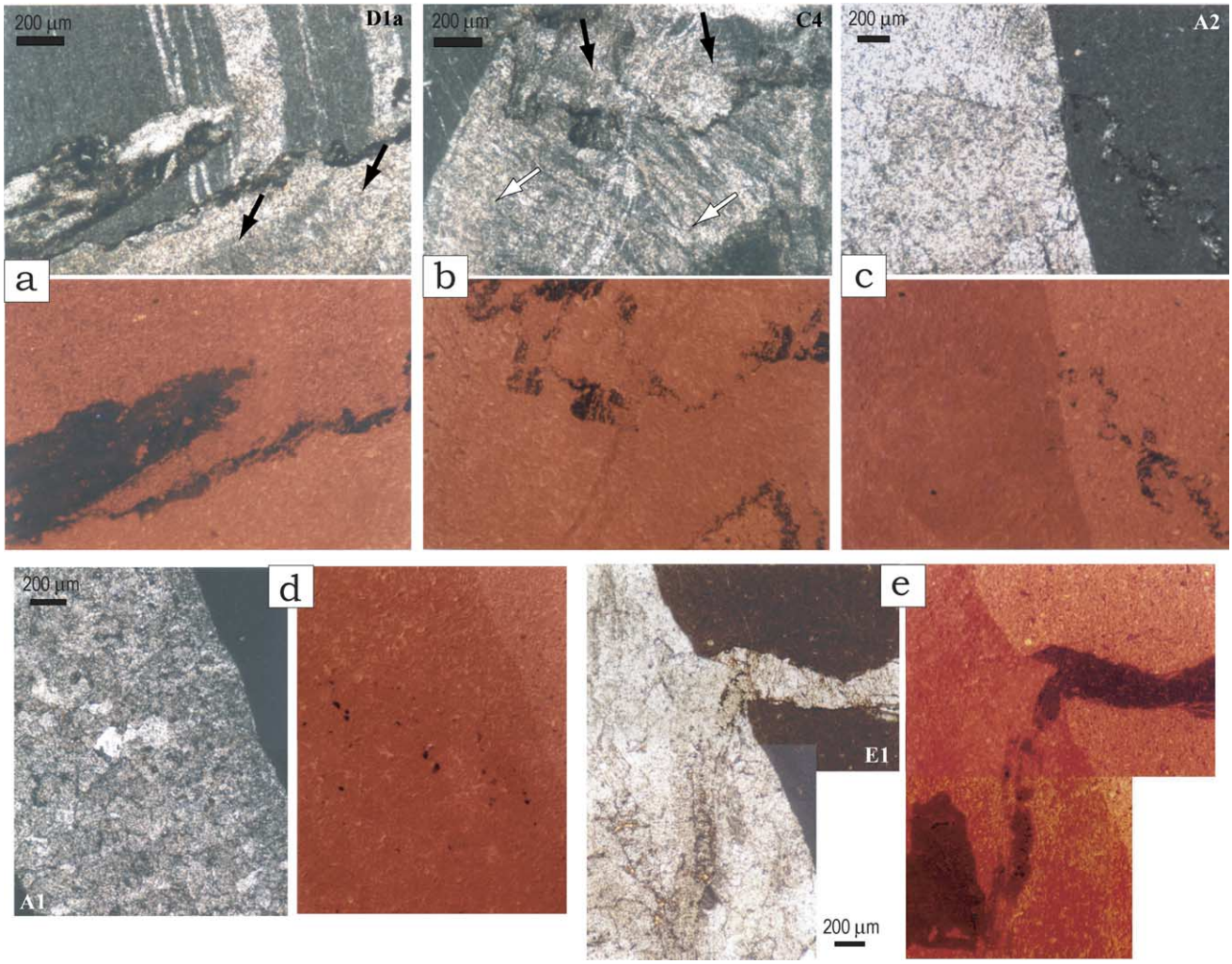

Fig. 6. Blégier site: cathodoluminescence (CL) microscopy. (a) The fibrous calcite characterizing a slip surface (black arrows) displays the same red luminescence as the host-limestone. Clayey minerals are dark-brown. (b) Stylolite surface bounding pull-apart calcite (top of the picture; black arrow) and a Type 2 fracture (white arrow). The two types of calcite and the limestone host-rock display the same CL-colour. (c) Calcite filling Type 1 fractures is dull-orange luminescent, a little darker than the host-limestones. (d) Calcite filling Type 2 fractures display the same red luminescence as the host-limestone. (e) Baroque dolomite is dark-brown to non-luminescent, and in places is related to or fills opened stylolite surfaces.

commonly higher than 80 °C (Alsharhan and Williams, 1987; Wojcik et al., 1993).

4.2. The La Remuque faults

4.2.1. Slip surfaces

Slip surfaces several tens of centimetres in length are the most evident features in the fault zones at the La Remuque site (Figs. 2c and 7a). They are more regular and straight than in the Blégier faults. They cut through several adjacent limestone layers and clay-rich interlayers, which are thus less dragged towards the slip surfaces than in the Blégier faults. Overlapping slip surfaces are connected by elongated calcite-filled dilational jogs (e.g. Sibson, 1989; Section 4.2.2). The main slip planes are characterized by layers a few millimetres thick showing thin calcite fibres (Fig. 7b). In places, stylolitic peaks testify combined shear and pressure solution processes (Peacock and Sanderson, 1995), but these features are rare if compared with those characterizing the Blégier slip surfaces. Slip surfaces are commonly characterized by abundant clay, or a clay/dolomite mixing (Fig. 7c). Rhomboidal, serrated, small crystals of dolomite related to recrystallization processes occur close to the slip surfaces (Fig. 7c). The fibrous calcite of the slip surfaces has red-orange luminescence under CL microscopy (Fig. 9a), similar to that of the host-limestone. Rhomboidal dolomite crystals are carmine-red luminescent, as well as the clay/dolomite mixing characterizing the slip surfaces (Fig. 9b).

4.2.2. Dilational jogs

In the La Remuque fault zones, a few elongated dilational jogs develop between the relatively long and straight, little spaced and overlapping, slip surfaces (Figs. 2 and 7a). They cut through limestone layers and therefore are not limited by clay-rich interlayers, as seen for the Blégier

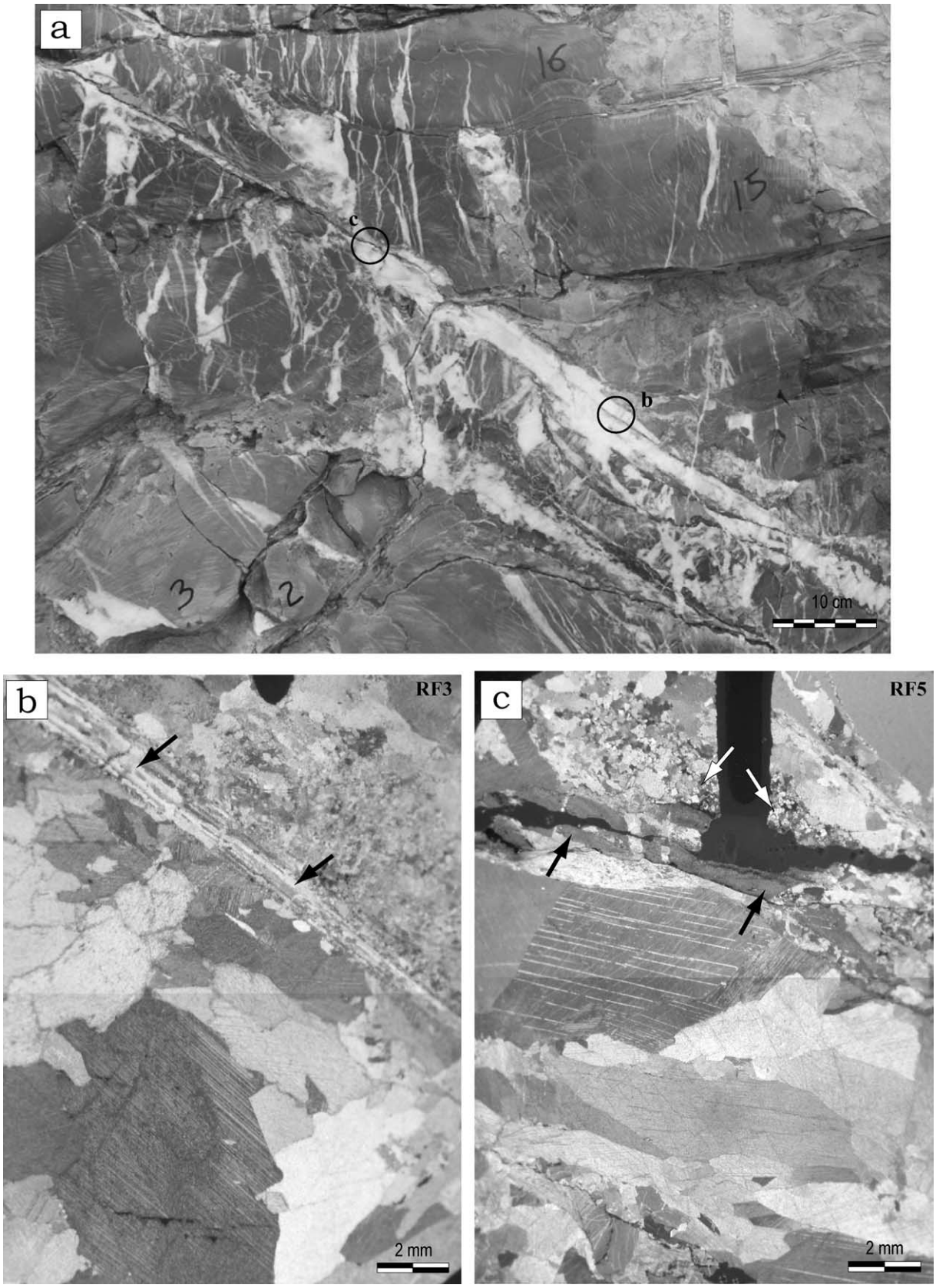

Fig. 7. Detailed images from the La Remuque site. (a) Closely spaced, overlapping, straight slip surfaces connected by elongated dilational jogs. Slip surfaces cut through several limestone layers and clay-rich interlayers (polished outcrop picture). The locations of Fig. 7b and c are shown. (b) Slip surface and a dilational jog. A layer a few millimetres thick with calcite fibres characterizes the slip surface (black arrow). The dilational jog (lower part of the picture) is

pull-aparts. Distances between consecutive dilational jogs along the fault zone are great and thus they never overlap. Dilational jogs only act as secondary structures connecting slip surfaces in developing the architecture of fault zones.

Dilational jogs are filled by euhedral–subhedral large blocky calcite crystals up to 10 mm in width (Fig. 7b and c). They display straight boundaries and are thinly twinned. Undulatory extinction or curved twin lamellae are not present. Calcite filling dilational jogs show strongly zoned luminescence. CL microscopy outlines the straight crystal boundaries (Fig. 9a and c). Zoned luminescence shows yellow, dark-yellow, dull-orange and dull-brown colours, characterizing different crystal growth steps and defining the individual facets of grains.

4.2.3. Type 1 fractures

Type 1 fractures are 1–10 mm in width, are perpendicular to the layer boundaries (Fig. 8a) and in general do not cross them. They affect the whole limestone rock with weak distribution relationships with the faults. Their strike is parallel to the fault strike-directions.

They are mostly constituted by euhedral–subhedral large calcite crystals (500 μm–2 mm wide; Fig. 8b), that are only weakly or not twinned and have straight grain boundaries. Small (50–100 μm) euhedral rhomboidal dolomite crystals are sporadically present in some veins, growing directly on the vein walls (Fig. 9d). These veins may be considered as equivalent to the Type 1 fractures of the Blégier site. Calcite filling the Type 1 fractures shows uniform red-rose luminescence, a little stronger (lighter) than the limestone host-rocks (Fig. 9d). Dolomite crystals are carmine-red luminescent and show an outer dull-red luminescent strip (Fig. 9d).

4.2.4. Flexural extensional fractures

Most of the calcite-filled fractures clustered along the slip surfaces may be interpreted as flexural extensional fractures, which in places have a triangular shape (Fig. 8c). They are not perfectly perpendicular to bedding and occur in the most deflected limestone layers close to the slip surfaces. Their strikes are scattered around the fault strike-direction. They are bounded by the clayey interlayers and their opening is consequently related to flexural slip mechanisms occurring between adjacent layers.

They are constituted by different calcite crystals: weakly twinned large crystals, elongated crystals and small drusy crystals with empty voids. No fibrous calcite is present (Fig. 8d). Under CL microscopy, calcite filling the flexural extensional veins is red-rose luminescent, a little stronger (lighter) than the limestone host-rocks.

4.2.5. Stylolitic surfaces

Late stylolites are strictly localized to within 10–20 cm of the slip surfaces, in particular in the most deflected and thinned limestone layers (Fig. 8e). This suggests that pressure solution processes are mostly related to a stress concentration controlled by the layering, as seen in the Blégier site (Section 4.1.5). Solution seams generally reuse the clay-rich interlayers present in the carbonate series. Late stylolitic surfaces do not appear to be coupled to the crystallization of the calcite filling the dilational jogs, rarely affecting or bounding this type of calcite.

5. Fluid inclusion data

Fluid inclusions within cements from the recognized microstructures were analyzed to define the *T*/*P* conditions of deformation during faulting. Fluid inclusions occurring in crystal growth zones were examined for the main microstructures. These fluid inclusions have a primary origin and are suitable for determining their trapping temperature (Goldstein and Reynolds, 1994). Less frequent secondary inclusions were also analyzed. A paleogeothermal gradient of 35°/km has been applied to correlate precipitation temperatures and depth from the isochores of the fluid inclusions. This thermal gradient has been obtained by Guilhaumou et al. (1996) based on fluid inclusion studies in the SE-Basin and geodynamic reconstruction for Cretaceous times. It is consistent with the values assumed for surrounding areas (Hermann Zeyen, pers. comm.; Barbarand et al., 2001; Séranne et al., 2002). Microthermometric measurements on other samples from the same survey sites gave similar and coherent results.

5.1. Blégier site

Petrographic analysis on samples F3b (coming from a pull-apart; Figs. 2a and 3d) and C2 (Type 1 fracture; Fig. 2a) revealed the presence of primary fluid inclusions (3–10 μm in size) with rounded, elongate and negative crystal shape. They are distributed along growth zones or in preferentially oriented groups in both fibrous and euhedral calcite crystals. Two-phase and mono-phase (all liquid) inclusions coexist. Baroque dolomite crystals show a high percentage of decrepitated inclusions (Fig. 10a), but some very small (2–5 μm) two-phase inclusions with consistent low percentages of vapour (5–10%) are present. Secondary fluid inclusions along healed microfractures are present. Ice melting temperatures (T_m; Fig. 11a) are typical of high salinity water with values around −11 and −20 °C (%NaCl weight eq.), perhaps containing various cations. Homogenization temperatures (T_h; Fig. 12a) were measured in calcite

filled by large euhedral–subhedral blocky calcite crystals. (c) Slip surfaces are characterized by a clay/dolomite mixing (black arrows) and rhomboidal, serrated crystals of dolomite (white arrows), related to re-crystallization processes. (b) and (c): crossed polarized photomicrographs.

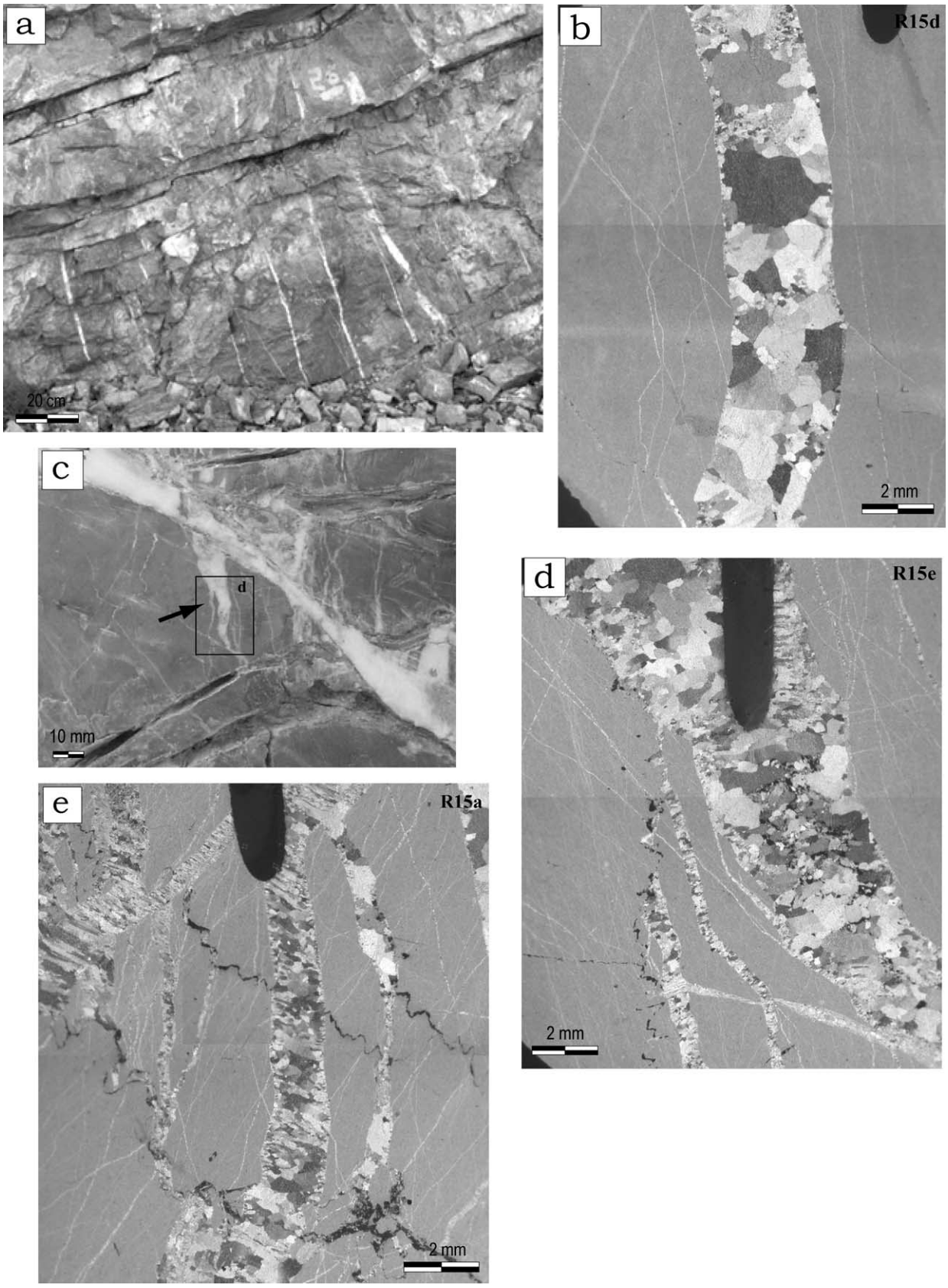

Fig. 8. La Remuque site. (a) Type 1 fractures are perpendicular to the stratification boundaries and in general do not cross them. (b) Large euhedral–subhedral calcite crystals fill Type 1 fractures, which opened perpendicularly to their walls. (c) Flexural extensional fractures show a triangular shape (black arrow) and are strictly localized in dragged layers close to the slip surfaces. (d) They are filled mostly by weakly twinned crystals and small drusy crystals. No fibrous

and baroque dolomite. They show mean values between 125 and 133 °C, with peak temperatures around 150 °C for primary inclusions and around 107 °C for secondary inclusions (sample C2).

5.2. La Remuque site

Samples RF3 (coming from a dilational jog; Figs. 2c and 7b) and R15d (Type 1 fracture; Figs. 2c and 8b) show many small primary mono- and two-phase fluid inclusions with well-defined shapes (Fig. 10b). Episodes of metastability during the heating/freezing runs were observed. Microthermometric data come from euhedral, in places twinned, crystals. Mean values for T_m are around −11/−15 °C (a few inclusions have a low salinity water content; Fig. 11b). Mean values for T_h are around 75 °C, with peak temperatures of 100 °C (Fig. 12b).

6. Stable isotope analysis

In the Blégier site, the $\delta^{18}O$ values of the bulk rock range from −4.08 to −4.39‰ relative to VPDB. The $\delta^{13}C$ values range from +2.78 to +2.90‰ VPDB. In the La Remuque site, the $\delta^{18}O$ values of the bulk rock vary between −0.79 and −3.12‰ VPDB. The $\delta^{13}C$ values range from +1.23 to +1.69‰ VPDB (Fig. 13). These values, although showing some variability, are consistent with the values reported for marine carbonates and Jurassic sedimentary rocks in the literature (e.g. Veizer and Hoefs, 1976; Hoefs, 1987; Travé et al., 1998; Kenis et al., 2000).

The calcite cements filling Blégier pull-aparts have $\delta^{18}O$ values varying between −4.94 to −5.61‰ VPDB and $\delta^{13}C$ values ranging from +2.72 to +2.81‰ VPDB. The calcite cements filling La Remuque dilational jogs have $\delta^{18}O$ values varying between −7.05 to −8.93‰ VPDB and $\delta^{13}C$ values ranging from +0.87 to −3.59‰ VPDB (Fig. 13).

In the Blégier fault zones, the similarity of the carbon isotopic compositions of the pull-aparts and of the surrounding limestone could be caused by precipitation of the calcite cements from a fluid in which carbon isotopic composition was buffered by the immediately adjacent surrounding rocks (Hudson, 1975; Gray et al., 1991; Marshall, 1992; Marquer and Burkhard, 1992; Muchez et al., 1995; Kenis et al., 2000). Pressure solution processes characterizing the clay-rich interlayer-derived slip surfaces that connect and bound the pull-aparts are likely to have provided the required calcium carbonate. From the $\delta^{18}O$ contents and using the temperature range derived from microthermometry (Section 5), the $\delta^{18}O$ of the parent solutions would be between +9 and +13‰ VSMOW. These values correspond to the highest observed for marine basin brines (e.g. Kharaka and Carothers, 1986).

In the La Remuque fault zones, the slightly difference between the $\delta^{13}C$ values of the cements in the dilational jogs and of those of the host-rock may reflect the contribution of a carbon source other than the immediately adjacent host-rocks and thus a relatively open system. The $\delta^{18}O$ values of these cements correspond to parent solutions with $\delta^{18}O$ varying from −2 to 0‰ VSMOW (precipitation at 50 °C) or from +4.5 to +6.5‰ VSMOW (precipitation at 100 °C). These values are close to that of seawater.

7. Discussion

7.1. Deformation mechanisms

Brittle fracturing and pressure solution/crystallization processes are the main deformation mechanisms acting in the studied fault zones. In both locations, limestone layers in the proximity of the slip surfaces are stretched and deflected by progressive intense fracturing and thinned by pressure solution processes, localized in bedding-parallel solution seams and in the clay-rich interlayers. Mineralized fractures are mainly located in the steps (Blégier pull-aparts and La Remuque dilational jogs) between slip surfaces and within the most deformed layers. They are filled by calcite showing different textures in the two studied sites. Pressure solution seams appear to dissolve more material in the Blégier fault zones than in the La Remuque ones. Mazzoli et al. (2004) suggest that low-temperature intracrystalline deformation could play a role in the formation of similar structures. Undulatory extinction and twinning in calcite and dolomite crystals mainly from the Blégier fault zones may be indicative of a component, though largely subordinate, of such a type of process.

7.2. Fracturing and evolution of fault zones

The spatial distribution of the microstructures, their cross-cutting relationships and the petrographic data can be synthesized into a two-dimensional model for the temporal evolution of the studied normal fault zones. Even if the studied faults affect the same sedimentary succession and are due to the same extensional tectonic event, the deformation characteristics are markedly different at the two sites. Deformation stages characterizing the proposed model are not necessarily synchronous in the two sites.

7.2.1. First deformation stage

At both survey sites, a first extensional phase is represented by the sub-vertical (when layers are rotated to the original horizontal attitude) Type 1 fractures (Figs. 14a and 15a; Sections 4.1.3 and 4.2.3). These veins have

calcite is present. (e) Stylolite surfaces are localized in the most dragged and thinned limestone layers, near to the slip surfaces. They reuse the pre-existing clay-rich interlayers. (a) and (c): polished outcrop pictures; (b), (d) and (e): crossed polarized photomicrographs.

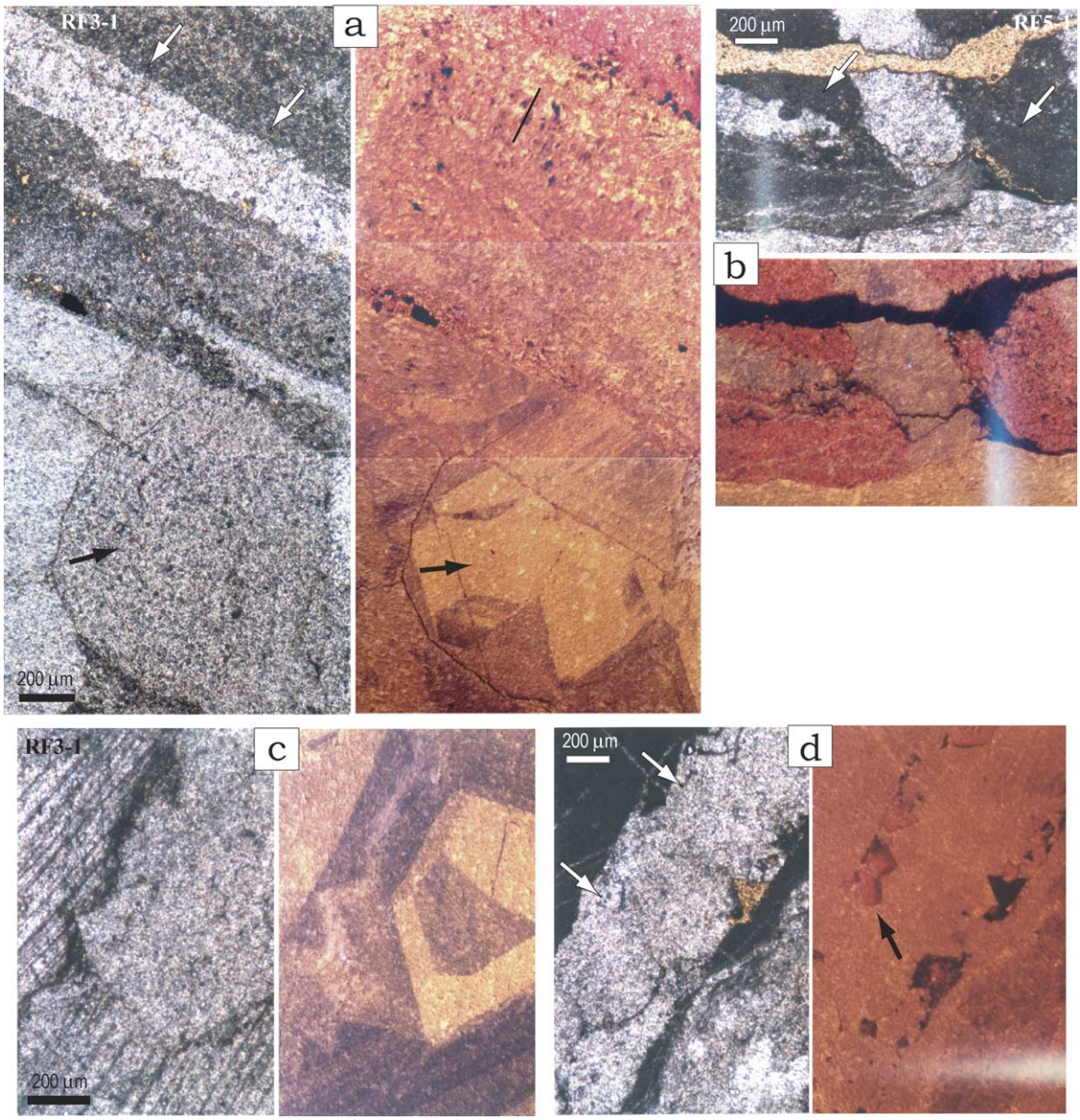

Fig. 9. La Remuque site: cathodoluminescence microscopy. (a) Slip surface (white arrows) and calcite filling a dilational jog (black arrow). Fibrous calcite characterizing the slip plane has red-orange luminescence as the host-limestone. The dilational jog calcite shows strongly zoned luminescence, suggesting slight fluctuations in fluid chemistry. (b) A clay/dolomite mixing (white arrows) commonly characterizes slip surfaces and is carmine-red luminescent. (c) Large, euhedral calcite crystals filling the dilational jogs display zoned yellow-brown luminescence. (d) Small, rhomboidal dolomite crystals (black arrow) are present in places in Type 1 fractures (white arrows) and are carmine-red luminescent.

large subhedral twinned crystals. They open perpendicularly to their walls, i.e. are mode I fractures. They strike parallel to the fault strikes, indicating that they are early structures related to the same stress field acting during fault development. They affect the whole outcrops and are not clustered around the faults (e.g. Fig. 8a). The CL-luminescence of calcite cements filling Type 1 fractures suggests fluid in chemical equilibrium with the limestone host-rock, in both the studied sites, which testifies rock–fluid interaction and local fluid circulation.

7.2.2. Second deformation stage

The second deformation stage shows different features at the two studied sites. In the Blégier site, most veins related to this stage are organized en-échelon, defining numerous shear zones that affect the whole limestone rock (Type 2 fractures; Fig. 14b; Section 4.1.4). Veins are filled mainly by fibrous calcite, which implies that filling took place during deformation (e.g. Ramsay and Huber, 1987; Hilgers and Urai, 2002). The opening at a low angle to the vein wall, as shown by fibre-vein wall angles and pre-existing offset structures, suggests that veins initiated as mixed

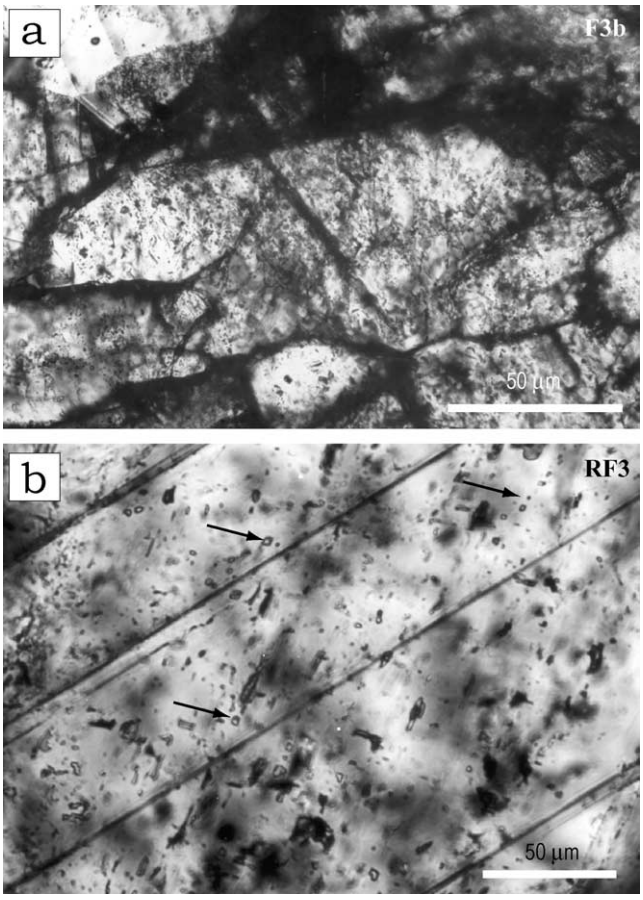

Fig. 10. Examples of analyzed fluid inclusions. (a) Baroque dolomite crystals from the Blégier site show a high percentage of decrepitated inclusions and some very small two-phase inclusions. (b) Small, rounded, two-phase, primary fluid inclusions (arrowed) in calcite from a dilational jog of the La Remuque site.

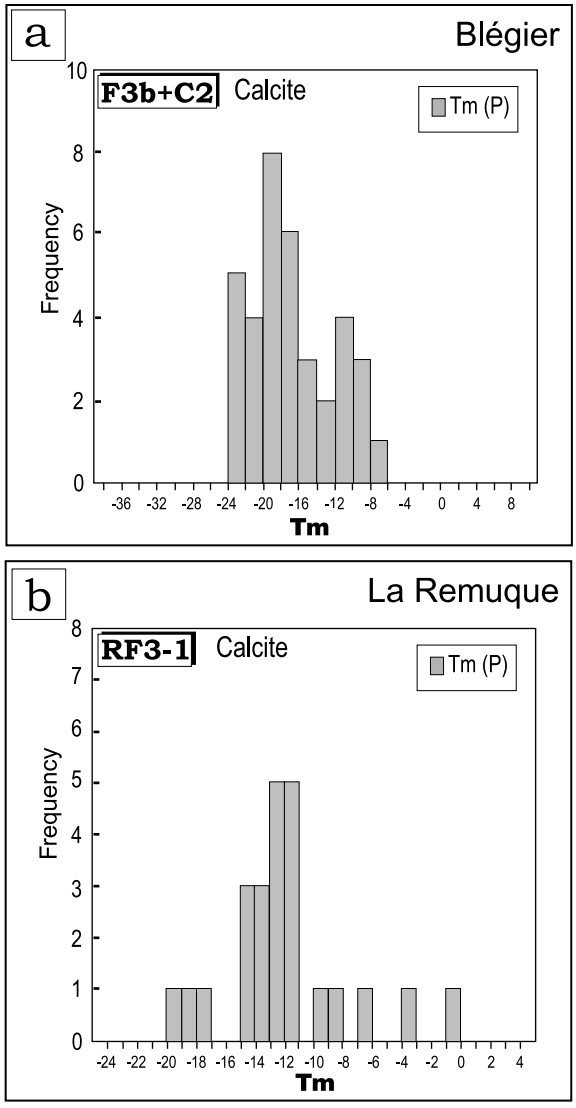

Fig. 11. Fluid inclusion microthermometry. Tm data (P: primary inclusions). (a) Blégier site: samples F3b (pull-apart calcite) and C2 (calcite near to a slip surface). (b) La Remuque site: sample RF3-1 (dilational jog calcite). At the Blégier site Tm are typical of high salinity water, whereas at the Remuque site Tm are less clustered, suggesting a relatively open system.

opening-shear fractures, and that there was shear displacement across each vein in this stage (e.g. McCoss, 1986; Petit et al., 1999). The shear displacement caused the first gentle bending of limestone layers.

En-échelon veins are not present in the La Remuque site (Fig. 15b). At this stage, incipient fault zones are characterized by a weak clustering of veins, which do not follow an en-échelon pattern. No fibrous calcite crystals are present. Most of these veins may be interpreted as flexural extensional fractures (Section 4.2.4) affecting some deformed and bent limestone layers at the tips of incipient slip surfaces. The early nucleation of slip surfaces may occur where the limestone layers show the most favourable properties to be easily fractured (e.g. due to layer thickness; Peacock and Sanderson, 1991) or there are pre-existing structures (e.g. Crider and Peacock, 2004).

En-échelon veins characterizing the Blégier site may be referred to as 'brittle–ductile' or 'semi-ductile' shear zones (e.g. Ramsay and Huber, 1987; Smith, 1997; Mazzoli and Di Bucci, 2003; Mazzoli et al., 2004). Peacock and Sanderson (1995), Willemse et al. (1997) and Crider and Peacock (2004) describe similar structures in the nucleation of strike-slip faults, which initiated as mode I vein arrays in the limestone beds. The role of en-échelon veins in nucleating and developing discrete fault zones by their coalescence, however, is limited at an early phase in the Blégier site. Such a phase is absent in the La Remuque site. In the Blégier site, en-échelon veins are early features reactivated during successive events (Section 7.2.3), whereas faults do not develop from such arrays in the La Remuque site.

All the types of fractures developed during the two first stages of deformation do not cross the clayey interlayers, at both studied sites. Moreover, they show CL colours similar to that of the limestone host-rock, in particular the fibrous veins in the Blégier site. This implies that fluid circulation

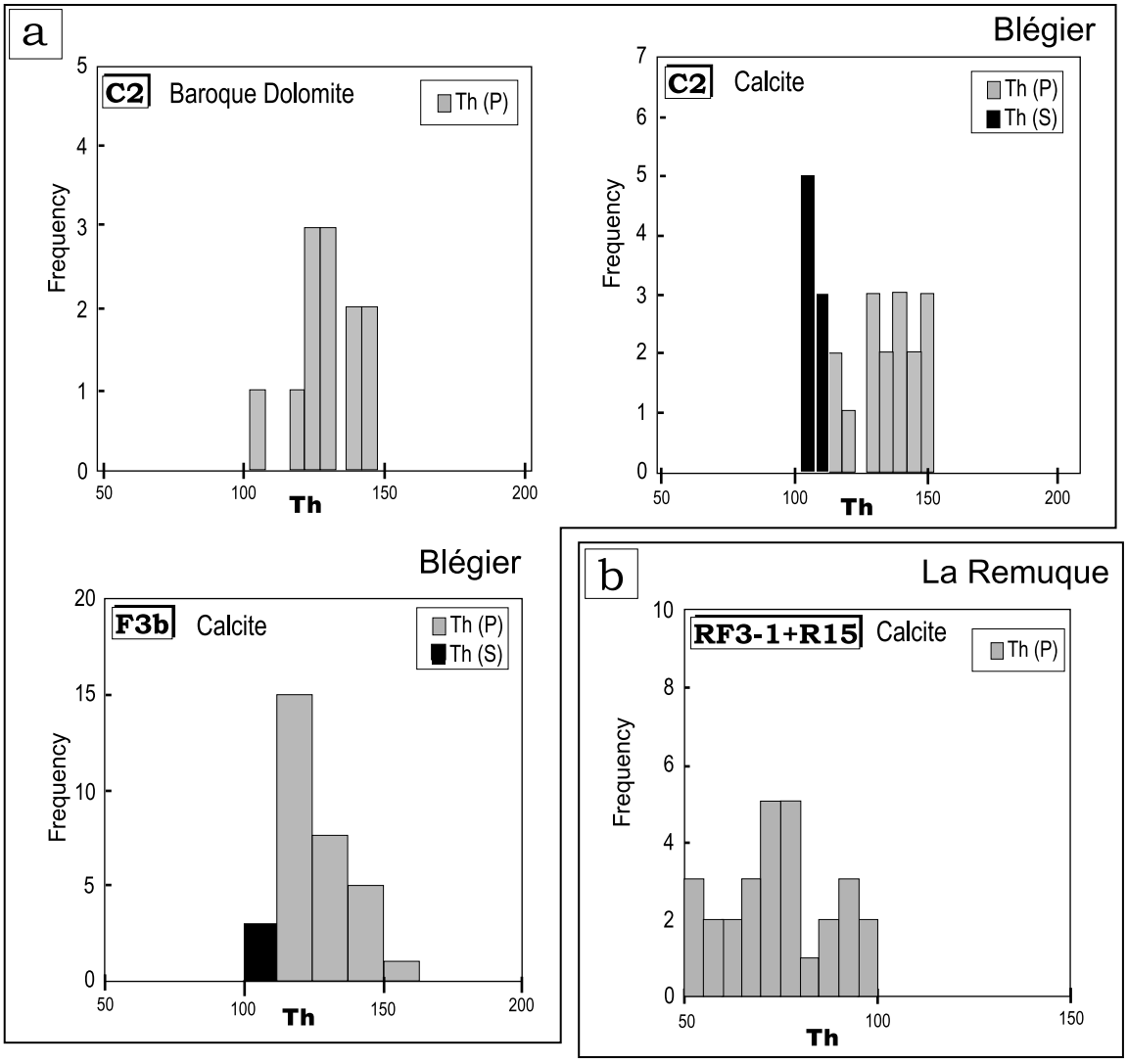

Fig. 12. Fluid inclusion microthermometry. Th data (P: primary inclusions; S: secondary inclusions). (a) Blégier: samples C2 (baroque dolomite and calcite in fractures near to a slip surface) and F3b (pull-apart calcite). (b) La Remuque: sample RF3-1 (dilational jog calcite) and R15 (Type 1 vein). Th values for primary inclusions from the Blégier site are higher than those at the La Remuque site, showing mean values of 130 and 75 °C, respectively.

was local, with limited mass transfer mainly from bed-parallel solution seams to the fractures opening within the same limestone layer.

7.2.3. Third deformation stage

The third stage is represented by discrete, segmented slip planes, with the re-activation and neo-formation of stylolites and the precipitation of calcite in pull-aparts and dilational jogs. These processes are concentrated near to the slip surfaces, where limestone layers are gradually thinned and dragged and disconnected into the fault zone, mostly by fracturing and pressure solution processes. Deformation styles are, however, clearly different in the two sites.

In the Blégier site, the fault zones are characterized by the formation of calcite-filled (locally baroque dolomite) pull-aparts (Fig. 14c and d; Section 4.1.2) allowing fault displacement to increase. They develop from en-échelon veins (Type 2 fibrous calcite-filled fractures; stage 2), as described for strike-slip fault zones (Peacock and Sanderson, 1995; Willemse et al., 1997; Kelly et al., 1998). Fibrous crystals growing at low angles to the fracture walls (e.g. 'crack-slip, then seal' model; Petit et al., 1999) show that shear displacement occurs across the vein arrays, which gently bends the limestone layers. As the veins widen, clay-rich interlayers, acting as pre-existing surfaces of weakness, are subjected to shear due to increased rotation and start to slip (Fig. 14c; Crider and Peacock, 2004). A pull-apart, and thus a distinct slip surface, forms when slip occurs on the solution seams that link a vein with adjacent vein segments. Pull-aparts connect (Fig. 14d) and merge as the slip increases, forming a composite pull-apart with continuous calcite fill (see central part of Fig. 2a and b).

There are some important differences between the model presented here and that shown by Willemse et al. (1997),

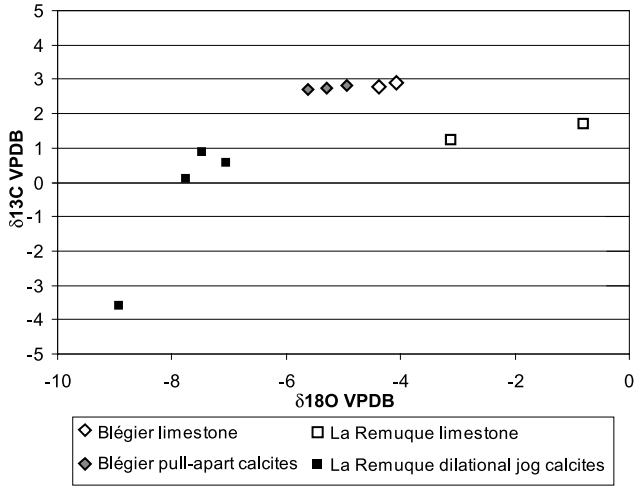

Fig. 13. Carbon and oxygen isotopic compositions of the limestone host-rocks and of the calcite cements filling pull-apart and dilational jog structures, respectively, from the Blégier and La Remuque sites. The data suggest that significant rock–fluid interaction occurred at both sites. At the La Remuque site, differences in carbon isotopic compositions could be related to a relatively open system.

who recognized the key role of pressure solution seams during the nucleation, growth and linkage of individual strike-slip fault segments. They proposed that several generations of solution seams hierarchically develop at one particular location on the fault zone. Stylolites of each of the various generations serve as preexisting discontinuities along which slip can occur. Our observations on normal faults do not recognize different generations of solution seams, but show that the pre-existing clay-rich interlayers continually localize shear. Early pressure solution processes and successive slip take place on the same surfaces (i.e. the clay-rich interlayers) during the nucleation and growth of slip planes. Also, Peacock and Sanderson (1995) described just one set of stylolites in developing strike-slip faults, but they were newly-formed and not reactivating clayey interlayers. The vertical fault plane segmentation in the Blégier faults is an outcome of the presence of originally sub-horizontal clayey discontinuities. Thus, slip surfaces initiated as clay-rich interlayers, acted mainly as pressure solution seams during the early stages of deformation, with slip only occurring later as limestone layers rotated and throws became more important.

The calcite filling the pull-aparts is bounded by and coupled with late sheared solution seams. It mostly consists of elongated, fibrous crystals that indicate their syntectonic growth (Section 4.1.2), and suggest that the deformation rate is slow compared with the rock solubility (Ramsay, 1980; Canole et al., 1997; Hilgers and Urai, 2002). Pull-apart calcite shows the same CL-luminescence as the host-limestone, suggesting fluid in chemical equilibrium with the limestone. No indication of CL-banding tracing individual calcite facets was observed. The development of facets and growth competition is suppressed if the opening of fractures is slow compared with the rock solubility (Urai et al., 1991; Hilgers et al., 2001). The similarity of the stable isotopic composition of the pull-apart calcite and of the surrounding limestone confirms the exchange between fluid and the immediately adjacent host-rocks. These observations suggest that mass transfer may become important in the fault zone, but the circulation is very local, with fluids in chemical equilibrium with the limestone host-rocks. The Blégier fault zones, developing at relatively high *P*/*T* conditions, may be considered to act as strictly closed systems to fluid circulation during their whole evolution.

The third deformation stage at La Remuque site is characterized by strain localized on relatively long discrete slip surfaces (Fig. 15c and d). The early slip surfaces, nucleated during stage 2, propagated upwards and downwards. Propagation, however, is likely to be vertically restricted by certain layers or bedding discontinuities, as described in layered sequences by several authors (e.g. Gross et al., 1997; Wilkins and Gross, 2002; Soliva and Benedicto, 2005). Vertical restriction occurs where the interface or adjacent layer inhibit propagation of the fault tip across the sequence (Nicol et al., 1996; Benedicto et al., 2003), or within homogeneous lithologies (as the limestone affected by the studied faults) separated by weak interfaces (Cooke and Underwood, 2001). In the La Remuque faults, clayey interlayers play a role in inhibiting slip surface propagation. Restriction induces bending of the not yet offset limestone layers toward the slip surfaces, causes opening or widening of flexural extensional fractures and enhances solution phenomena localized in the clay-rich interlayers (Fig. 15c). As deformation continues, a single slip surface can cross the preventing interface/bed or connect to an adjacent slip surface by the formation of a calcite-filled dilational jog as a result of the breakage and dislocation of the layer between the adjacent slip surface tips (Fig. 15d).

Dilational jogs at La Remuque do not develop by widening of the stage 2 veins and do not characterize the most deformed layers, as seen for pull-aparts in Blégier. Slip surfaces do not initiate in clay-rich interlayers, but cut through them. They are newly-formed features.

The calcite within dilational jogs consists of large, euhedral crystals that filled a cavity that probably opened by high rate displacement (Gratier and Gamond, 1990; Canole et al., 1997). Crystals have few twins, indicating weak deformation (Burkhard, 1993). CL-gradients outlining the facets of individual grains suggest fluctuations in fluid chemistry and crystals growing in free fluid (Sommer, 1972; ten Have and Heijnen, 1985; Dromgoole and Walter, 1990; Travé et al., 1998). Petrographic and geochemical data suggest that the dilational jogs could remain open until they are filled by calcite crystals growing in free-fluid conditions, with slight fluctuations in fluid chemistry. In the La Remuque fault zones, therefore, the third stage of deformation allows fluid circulation to relatively increase, as slip surfaces connect to one another by the opening of dilational jogs.

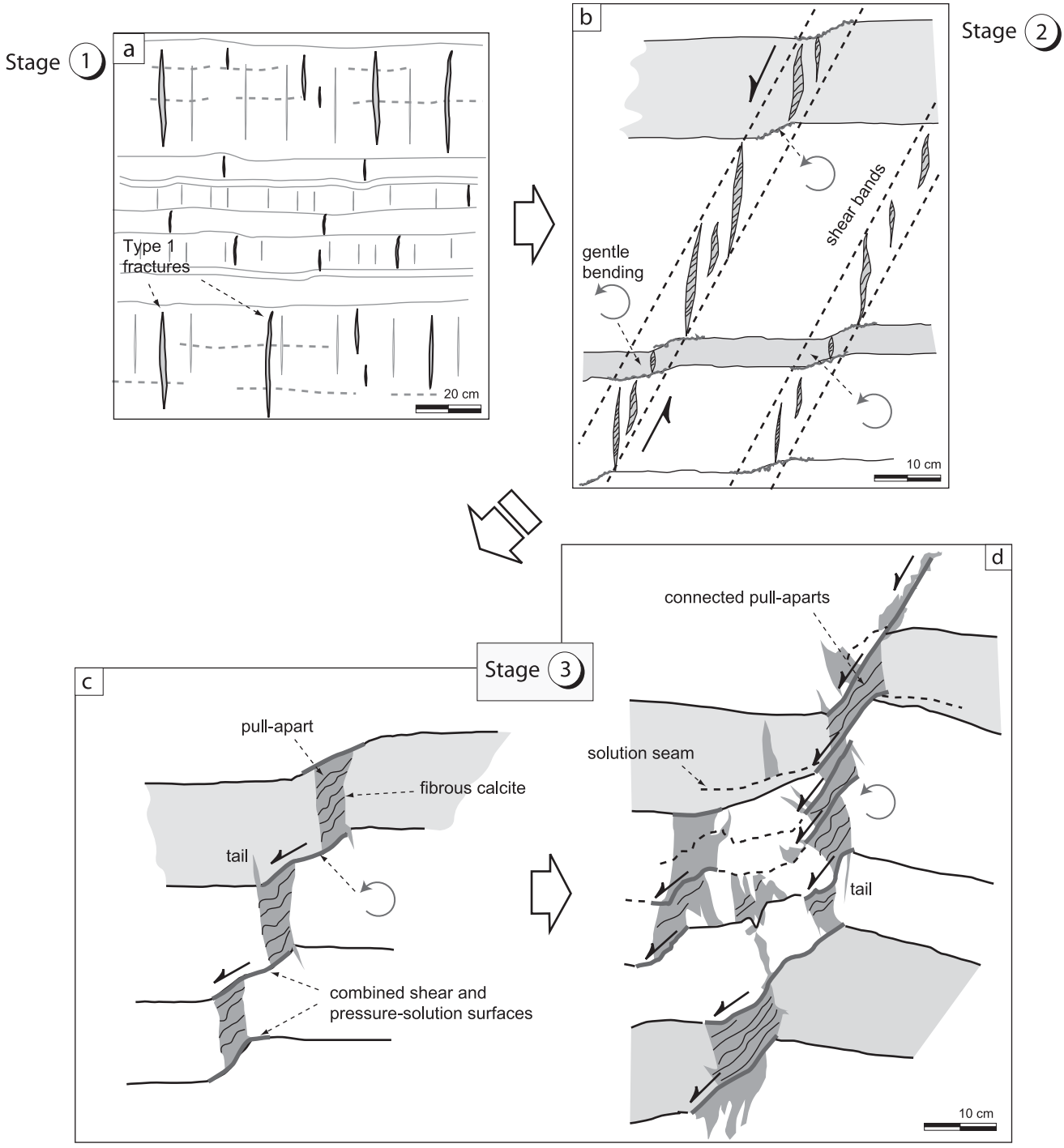

Fig. 14. Model for the development of normal fault zones in the Blégier site (sketch scales are approximate). (a) Stage 1: sub-vertical mode I fractures (Type 1 fractures) constituted by large subhedral twinned crystals. (b) Stage 2: en-échelon fracture (Type 2 fractures) arrays affecting the whole limestone rock. Veins are filled mainly by fibrous calcite crystals. The limestone layers are gently bent because of the vein opening at a low angle to their walls. Stage 3: (c) as the veins widen, clay-rich interlayers are subjected to shear due to increased rotation and start to slip. (d) Well-developed pull-aparts are filled by elongated, fibrous calcite. Displacement along the slip surfaces is sufficient to link them. Pressure solution processes localize on slip surfaces and lead the limestone layers to be thinned in the fault zone.

7.3. Role of P/T conditions on deformation characteristics

The studied faults affect the 'Barre Tithonique' at the same stratigraphic level, showing quite homogeneous and similar lithological characteristics in both survey sites. They are related to the same weak extensional tectonic phase. Deformation styles are, however, substantially different in the Blégier and La Remuque sites, as seen above.

The calcite crystals filling the pull-aparts of the Blégier fault zones in places show thick and curved twin lamellae,

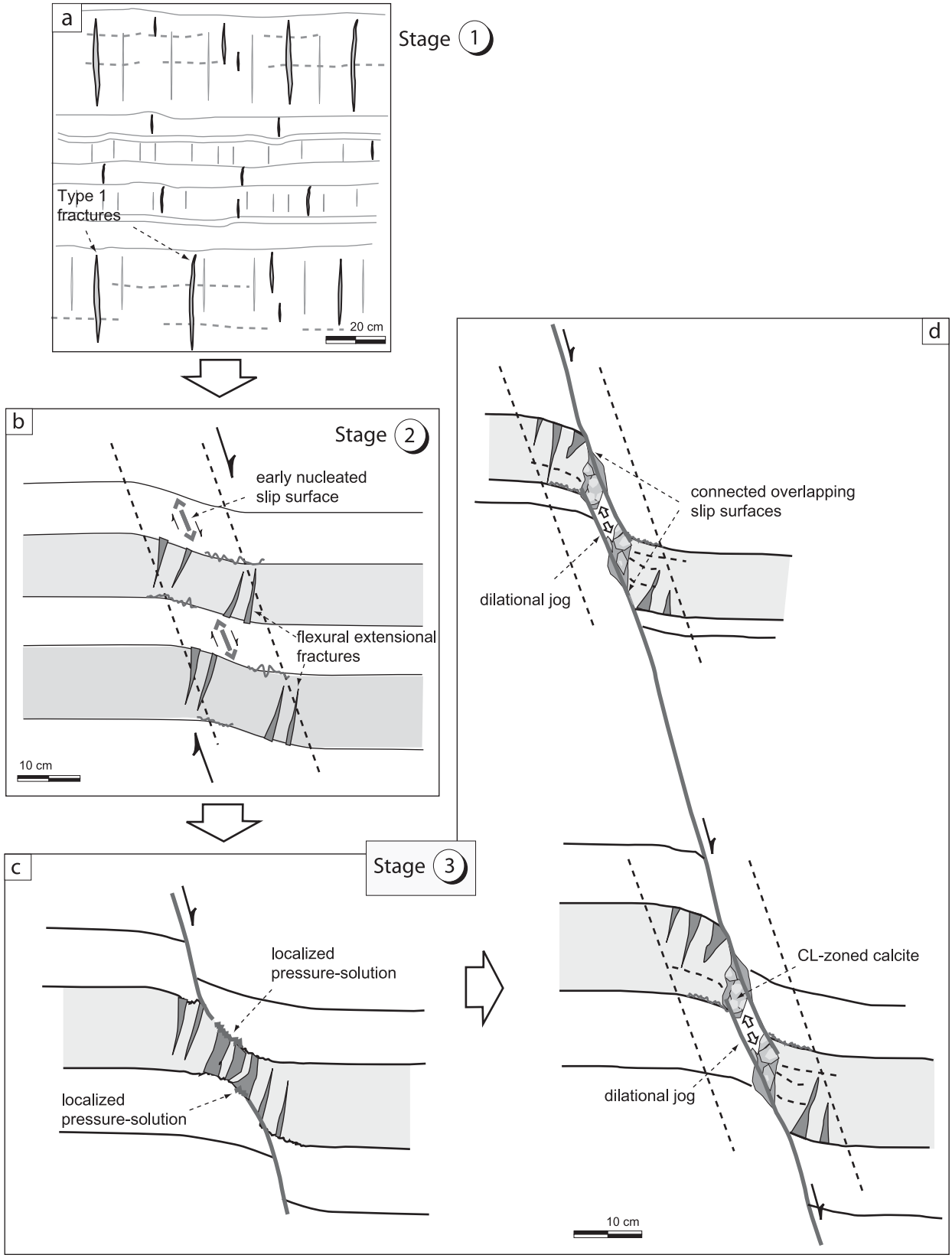

Fig. 15. Model for the development of normal fault zones in the La Remuque site (sketch scales are approximate). (a) Stage 1: sub-vertical mode I fractures (Type 1 fractures) constituted by large subhedral twinned crystals. (b) Stage 2: early nucleation of incipient slip surfaces. Deformed and bent limestone layers along incipient slip surfaces are affected by flexural extensional fractures. No fibrous calcite is present. Stage 3: (c) the clay-rich interlayers inhibit slip surface propagation, which leads to the widening of fractures and localization of the solution phenomena. (d) As deformation continues, a single slip surface crosses the preventing interface and can connect to an adjacent slip surface by the formation of a CL-zoned calcite-filled dilational jog.

possibly related to an intense deformation and relatively high temperatures. In the Blégier calcite- and baroque dolomite-filled fractures, the mean values of the homogenization temperature (T_h) measured for two-phase primary fluid inclusions range from 125 to 133 °C. In the La Remuque site, T_h in calcite-filled fractures are lower, with mean values around 75 °C. T_h for each site were also measured in microstructures far away from the fault zones. CL microscopy and stable isotope analyses confirm fluids in chemical equilibrium with the host-limestones in the Blégier site, where higher T_h were measured. This suggests a very local circulation of fluids, as confirmed also by the ice melting temperature values (T_m), with no evidence of hydrothermal alteration. In both sites, fluid migrating from depth along the faults is unlikely. The most probable cause for the relatively high T_h in primary fluid inclusions is therefore the depth at which fault-related structures developed. Taking into account a geothermal gradient of 35°/km, the difference of the measured T_h corresponds to a difference in depth of 1.5–2 km (mean value 1.65 km). We suggest that the different depth of deformation for the two studied sites is related to the different regional subsidence during Cretaceous times, as described in Section 2.

Relatively high P/T conditions at the Blégier site ($T>$ 120 °C; depth ~2.9–3.6 km) enhance the development of en-échelon veins and slip surface-related pull-aparts, which are progressively filled by fibrous calcite crystals without formation of voids. Moreover, the efficiency of dissolution/crystallization in limestone is enhanced by low strain rates and fracture-related, local fluid circulation (Rutter, 1976). Formation of 'brittle–ductile' shear zones, characterized by en-échelon, calcite-filled veins may be enhanced by relatively high P/T conditions (Smith, 1997; Willemse et al., 1997; Mazzoli and Di Bucci, 2003).

In contrast, relatively low P/T conditions at La Remuque site ($T<90$ °C; depth ~1.5–2 km) favour the early nucleation of slip surfaces. These propagate by cutting through limestone layers. Long stepped slip surfaces may connect with one another via dilation jogs. Brittle deformation, relatively fast compared with crystallization rate, lets dilational jogs open with the formation of voids, until they are filled by large euhedral calcite crystals, growing in free-fluid conditions, as shown by CL zoning. Relatively low P/T conditions enhance brittle processes with respect to pressure solution phenomena, allowing slip surfaces to develop early and segment weakly, with a minor role played by dilational jogs.

8. Conclusions

This study provides macro- and microanalyses of the style of early stages of normal faulting in natural vertical cliffs in limestone rocks. The originality of this work is the detailed microstructural analysis, integrating different methodologies, of the structures characterizing each stage of the initiation of normal faults. We provide two different models for the evolution of the studied normal faults, which we relate to the P/T conditions.

Field, petrographic, stable isotope and fluid inclusion data from small-offset normal faults affecting the Tithonian limestones of the French SE-Basin allowed us to recognize different structural evolutions in the two studied sites, after a common first stage characterized by sub-vertical mode I fractures. In the Blégier site, deformation localizes along shear zones defined by en-échelon, fibrous calcite-filled fractures. Progressive opening of fractures and deflecting of limestone layers lead to the formation of adjacent pull-aparts connected by short slip surfaces. Slip surfaces systematically develop on clayey interlayers and rarely cross through the limestone layers. They bound the pull-aparts, which are filled by syntectonic fibrous calcite. In contrast, at the La Remuque site the incipient fault zones are characterized by an early nucleation of slip surfaces. Vertical restriction in slip surface propagation leads some limestone layers to bend at slip surface tips, and enhances pressure solution processes on clay-rich layer boundaries. As the slip surfaces propagate across the layers, they can connect with adjacent overlapping surfaces by dilation jogs that are filled by large euhedral calcite crystals, growing in free-fluid conditions. Slip surfaces finally cut through several limestone layers.

Our study shows that the clay-rich interlayers characterizing the carbonate series in both studied sites play a major role during deformation. In the Blégier fault zones, they act as preexisting surfaces where pressure solution phenomena localize, and then shear and slip develop, as deformation increases and the layers rotate. In the La Remuque fault zones, they take part in the restriction of slip surface propagation and thus in fault plane segmentation. Our study also shows that the differences in the style of initial stages of faulting in the two studied sites are related mainly to the P/T conditions, i.e. the depth at which the fault zones developed. Depth is therefore the primary control in defining the relative importance of the different deformation mechanisms in limestones, such as brittle fracturing and pressure solution processes. The Blégier fault zones developed at higher P/T conditions, causing all fault-related fractures to be progressively filled by fibrous calcite, as they opened. Fluid circulation was local and fluids were in chemical equilibrium with the host-rocks. In the La Remuque fault zones that developed at a shallower depth, long slip surfaces propagated and connected with one another by means of dilational jogs. These remained temporarily open and let fluid flow relatively increase with slight fluctuations in fluid chemistry.

Acknowledgements

This work has been carried out in the frame of a research convention TOTAL-Universitè Paris XI

(DGEP/TDO/CA/RD n.12806A1/UPS n. 60521/CNRS: 041.1883.01). We thank Sylvie Delisle and Jean-Loup Montenat for the facilities and the helpful discussions. We thank Frederic Bouchette and Maurice Pagel for the cordial suggestions on the outcrop structures and petrographic data, and Hermann Zeyen for his insights into geophysical data. We thank Jean-Pierre Villotte and Aldo Marchionni for the preparation of thin and polished sections, and Maura Bussolotto, Elena Crespi, Alban Duriez and Marina Gillon for the help on isotope and fluid inclusion analyses. The reviews of Stefano Mazzoli and Neil Mancktelow and the very constructive comments of David Peacock significantly improved the manuscript.

References

Alsharhan, A.S., Williams, D.F., 1987. Petrography and stable isotope composition of baroque dolomite from the Shuaiba formation (Lower Cretaceous), Abu Dhabi, United Arab Emirates. Journal of African Earth Sciences 6, 881–890.

Ballesio, M., Flandrin, J., Moullade, M., Porthault, B., Truc, G., 1975. Notice explicative. Carte Géologique de la France, feuille NYONS (891). Orléans: Bureau de Recherches Géologiques et Minières, p. 19. Scale. 1:50,000.

Barbarand, J., Lucazeau, F., Pagel, M., Séranne, M., 2001. Burial and exhumation history of the south-eastern Massif Central (France) constrained by apatite fission-track thermochronology. Tectonophysics 335, 275–290.

Benedicto, A., Schultz, R.A., Soliva, R., 2003. Layer thickness and the shape of faults. Geophysical Research Letters 20, 2076.

Bouchette, F., Séguret, M., Moussine-Pouchkine, A., 2001. Coarse carbonate breccia as the result of water-wave cyclic loading (uppermost Jurassic–South East Basin, France). Sedimentology 48 (4), 767–789.

Burkhard, M., 1993. Calcite twins, their geometry, appearance and significance as stress–strain markers and indicators of tectonic regime: a review. Journal of Structural Geology 15, 351–368.

Canole, P., Odonne, F., Polve, M., 1997. Heterogeneous strain associated with normal faulting: evidence of mass transfer by pressure solution associated with fault displacement. Tectonophysics 283, 129–143.

Cooke, M.L., Underwood, C.A., 2001. Fracture termination and step-over at bedding interfaces due to frictional slip and interface opening. Journal of Structural Geology 23, 223–238.

Craig, H., 1957. Isotope standards for carbon and oxygen and correction factors for mass-spectrometric analysis of carbon dioxide. Geochimica et Cosmochimica Acta 12, 133–149.

Crider, J.G., Peacock, D.C.P., 2004. Initiation of brittle faults in the upper crust: a review of field observation. Journal of Structural Geology 26, 691–707.

Cros, P., Lanau, P., Vinchon, C., Bonhomme, M.G., Boulègue, L., Cula, P., Giot, D., 1993. Sandstone diagenesis and evolution of the porosity in a potential Triassic source rock (Privas area, Ardèche). Bullettin de la Société Géologique de France 164, 631–647.

De Graciansky, P.C., Dardeau, G., Dumont, T., Jacquin, T., Marchand, D., Mouterde, R., Vail, P.R., 1993. Depositional sequence cycles, transgresive-regressive facies cycles, and extensional tectonics: examples from the southern Subalpine Jurassic basin, France. Bullettin de la Société Géologique de France 16, 709–718.

Debrand-Passard, S., Courbouleix, S., 1984. Synthèse géologique du Sud-Est de la France. Mémoire BRGM Fr., no. 126.

Dercourt, J., Ricou, L.E., Vrielynck, B.E., 1993. Atlas Téthys Palaeoenvironmental Maps. Gauthiers-Villars, Paris.

Dromgoole, E.L., Walter, L.M., 1990. Iron and manganese incorporation into calcite: effects of growth kinetics, temperature and solution chemistry. Chemical Geology 81, 311–336.

Franssen, R.C.M.W., Peach, C.J., Willemse, E.J.M., 1994. Fault sealing mechanisms in sandstones. In: 1994 AAPG Annual Meeting, Denver, American Association of Petroleum Geologists. p. 151.

Gignoux, M., Moret, J., 1938. Géologie Dauphinoise, 1st ed Masson, Paris. 391pp.

Goldstein, R., Reynolds, J., 1994. Systematics of fluid inclusions in diagenetic minerals. Society for Sedimentary Geology. Short Course 31.

Gratier, J.P., Gamond, J.F., 1990. Transition between seismic and aseismic deformation in the upper crust. In: Knipe, R.J., Rutter, E.H. (Eds.), Deformation Mechanisms, Rheology and Tectonics Geological Society of London Special Publication, vol. 54.

Gray, D.R., Gregory, R.T., Durney, D.W., 1991. Rock-buffered fluid-rock interaction in deformed quartz-rich turbidite sequences, Eastern Australia. Journal of Geophysical Researcher 96, 19681–19704.

Gross, M.R., Gutierrez-Alonzo, G., Bai, T., Wacker, M.A., Collinsworth, K.B., Behl, R.J., 1997. Influence of mechanical stratigraphy and kinematics on fault scaling relations. Journal of Structural Geology 19, 171–183.

Guilhaumou, N., Touray, J.C., Perthuisot, V., Roure, F., 1996. Palaeo-circulation in the basin of southeastern France sub-alpine range: a synthesis from fluid inclusions studies. Marine and Petroleum Geology 6, 695–706.

Haccard, D., Beaudoin, B., Gigot, P., Jorda, M., 1989. Notice explicative. Carte Géologique de la France, feuille LA JAVIE (918). Orléans: Bureau de Recherches Géologiques et Minières, Scale. 1:50,000. p. 152.

Hesthammer, J., Fossen, H., 2000. Uncertainties associated with fault sealing analysis. Petroleum Geoscience 6, 37–45.

Hilgers, C., Urai, J.L., 2002. Microstructural observation of natural syntectonic fibrous veins: implications for the growth process. Tectonophysics 352, 257–274.

Hilgers, C., Koehn, D., Bons, P.D., Urai, J.L., 2001. Development of crystal morphology during unitaxial growth in a progressively widening vein: II. Numerical simulations of the evolution of antitaxial fibrous veins. Journal of Structural Geology 23, 873–885.

Hoefs, J., 1987. Stable Isotope Geochemistry. Springer, Berlin.

Hudson, J.D., 1975. Carbon isotopes and limestone cement. Geology 3, 18–22.

Kelly, P.G., Sanderson, D.J., Peacock, D.C.P., 1998. Linkage and evolution of conjugate strike-slip fault zones in limestones of Somerset and Northumbria. Journal of Structural Geology 20, 1477–1493.

Kenis, I., Muchez, Ph., Sintubin, M., Mansy, J.L., Lacquement, F., 2000. The use of a combined structural, stable isotope and fluid inclusion study to constrain the kinematic history at the northern Variscan front zone (Bettechies, northern France). Journal of Structural Geology 22, 589–602.

Kharaka, Y.K., Carothers, W.W., 1986. Oxygen and hydrogen isotope geochemistry of deep basin brines. In: Fritz, P., Fontes, J.Ch. (Eds.), Handbook of Environmental Isotope Geochemistry. vol. 2: The Terrestrial Environment. Elsevier, pp. 305–360.

Knipe, R.J., 1997. Juxtaposition and seal diagrams to help analyze fault seals in hydrocarbon reservoirs. American Association of Petroleum Geologists Bulletin 81, 187–195.

Maltman, A.J., 1994. Prelithification deformation. In: Hancock, P.L. (Ed.), Continental Deformation. Pergamon, New York.

Marquer, D., Burkhard, M., 1992. Fluid circulation, progressive deformation and mass-transfer processes in the upper crust: the example of basement-cover relationships in the External Crystalline Massifs, Switzerland. Journal of Structural Geology 14, 1047–1057.

Marshall, D.J., 1988. Cathodoluminescence of Geologic Materials. Unwin Hyman, Boston, MA.

Marshall, J.D., 1992. Climatic and oceanographic isotopic signals from the carbonate rock record and their preservation. Geological Magazine 129, 143–160.

Mazzoli, S., Di Bucci, D., 2003. Critical displacement for normal fault nucleation from en-échelon vein arrays in limestones: a case study from the southern Apennines (Italy). Journal of Structural Geology 25, 1011–1020.

Mazzoli, S., Invernizzi, C., Marchegiani, L., Mattioni, L., Cello, G., 2004. 'Brittle-ductile' shear zone evolution and fault initiation in limestones, Monte Cugnone (Lucania), southern Apennines, Italy. In: Alsop, G.I., Holdsworth, R.E., McCaffrey, K.J.W., Hand, M. (Eds.), Flow Processes in Faults and Shear Zones Geological Society of London Special Publication, vol. 224, pp. 353–373.

McCoss, A.M., 1986. Simple constructions for deformation in transpression/transtension zones. Journal of Structural Geology 8, 715–718.

Menendez, B., Zhu, W., Wong, T., 1996. Micromechanics of brittle faulting and cataclastic flow in Brea sandstone. Journal of Structural Geology 18, 1–16.

Moore, D.E., Lockner, D.A., 1995. The role of microcracking in shear-fracture propagation in granite. Journal of Structural Geology 17, 95–114.

Muchez, Ph., Slobodnik, M., Viaene, W., Keppens, E., 1995. Geochemical constraints on the origin and migration of palaeo-fluids at the northern margin of the Variscan foreland, southern Belgium. Sedimentary Geology 96, 191–200.

Nicol, A., Watterson, J., Walsh, J.J., Childs, C., 1996. The shapes, major axis orientations and displacement patterns of fault surfaces. Journal of Structural Geology 18, 235–248.

Pagel, M., Barbin, V., Blanc, P., Ohnenstetter, D., 2000. Cathodoluminescence in Geosciences. Springer, Berlin.

Peacock, D.C.P., Sanderson, D.J., 1991. Displacement, segment linkage and relay ramps in normal fault zones. Journal of Structural Geology 13, 721–733.

Peacock, D.C.P., Sanderson, D.J., 1995. Pull-aparts, shear fractures and pressure solution. Tectonophysics 241, 1–13.

Peacock, D.C.P., Zhang, X., 1994. Field examples and numerical modelling of oversteps and bends along normal faults in cross-section. Tectonophysics 234, 147–167.

Petit, J.P., Wibberley, C.A.J., Ruiz, G., 1999. 'Crack-seal', slip: a new fault valve mechanism? Journal of Structural Geology 21, 1199–1207.

Ramsay, J.G., 1980. The crack-seal mechanism of rock deformation. Nature 284, 135–139.

Ramsay, J.G., Graham, R.H., 1970. Strain variations in shear belts. Canadian Journal of Earth Sciences 7, 783–813.

Ramsay, J.G., Huber, M.I., 1987. The Techniques of Modern Structural Geology, Fold and Fractures, vol. 2. Academic Press, London.

Roure, F., Brun, J.P., Colletta, B., Vially, R., 1994. Multiphase extensional structures, fault reactivation and petroleum plays in the alpine foreland basin of southeastern France. In: Mascle, A. (Ed.), Hydrocarbon and Petroleum Geology of France Special Publication. Springer, New York, pp. 245–248.

Rutter, E.H., 1976. The kinetics of rock deformation by pressure solution. Philosophical Transactions of Royal Society of London 283, 203–219.

Séguret, M., Moussine-Pouchkine, A., Raja Gabaglia, G., Bouchette, F., 2001. Storm deposits and storm-generated coarse breccias on a pelagic outer-shelf (South East Basin, France). Sedimentology 48 (2), 231–254.

Séranne, M., Camus, H., Lucazeau, F., Barbarand, J., Quinif, Y., 2002. Surrection et érosion polyphasées de la Bordure cévenole. Un example de morphogenèse lente. Bullettin de la Société Géologique de France 173, 97–112.

Sibson, R.H., 1989. Earthquake faulting as a structural process. Journal of Structural Geology 11, 1–14.

Smith, J.V., 1997. Initiation of convergent extension fracture vein arrays by displacement of discontinuous fault segments. Journal of Structural Geology 19, 1369–1373.

Soliva, R., Benedicto, A., 2005. Geometry, scaling relations and spacing of vertically restricted normal faults. Journal of Structural Geology 27, 317–325.

Sommer, S.E., 1972. Cathodoluminescence in carbonates, 1. Characterization of cathodoluminescence from carbonate solid solution. Chemical Geology 9, 257–273.

ten Have, T., Heijnen, W., 1985. Cathodoluminescence activation and zonation in carbonate rocks: an experimental approach. Geologie en Mijnbouw 64, 297–310.

Travé, A., Calvet, F., Soler, A., Labaume, P., 1998. Fracturing and fluid migration during Palaeogene compression and Neogene extension in the Catalan Coastal Ranges, Spain. Sedimentology 45, 1063–1082.

Urai, J.L., Williams, P.F., van Roermund, H.L.M., 1991. Kinematics of crystal growth in syntectonic fibrous veins. Journal of Structural Geology 13, 823–836.

Veizer, J., Hoefs, J., 1976. The nature of O^{18}/O^{16} and C^{13}/C^{12} secular trends in sedimentary carbonate rocks. Geochimica et Cosmochimica Acta 40, 1387–1395.

Wilkins, S.J., Gross, M.R., 2002. Normal fault growth in layered rocks at Split Mountain, Utah. Journal of Structural Geology 24, 1413–1429.

Willemse, E.J.M., Peacock, D.C.P., Aydin, A., 1997. Nucleation and growth of strike-slip faults in limestones from Somerset, UK. Journal of Structural Geology 19, 1461–1477.

Wojcik, K.M., Goldstein, R.H., Walton, A.V., 1994. History of diagenetic fluids in a distant foreland area, Middle and Upper Pennsylvanian, Cherokee basin, Kansas, USA: fluid inclusion evidence. Geochimica et Cosmochimica Acta 58, 1175–1191.